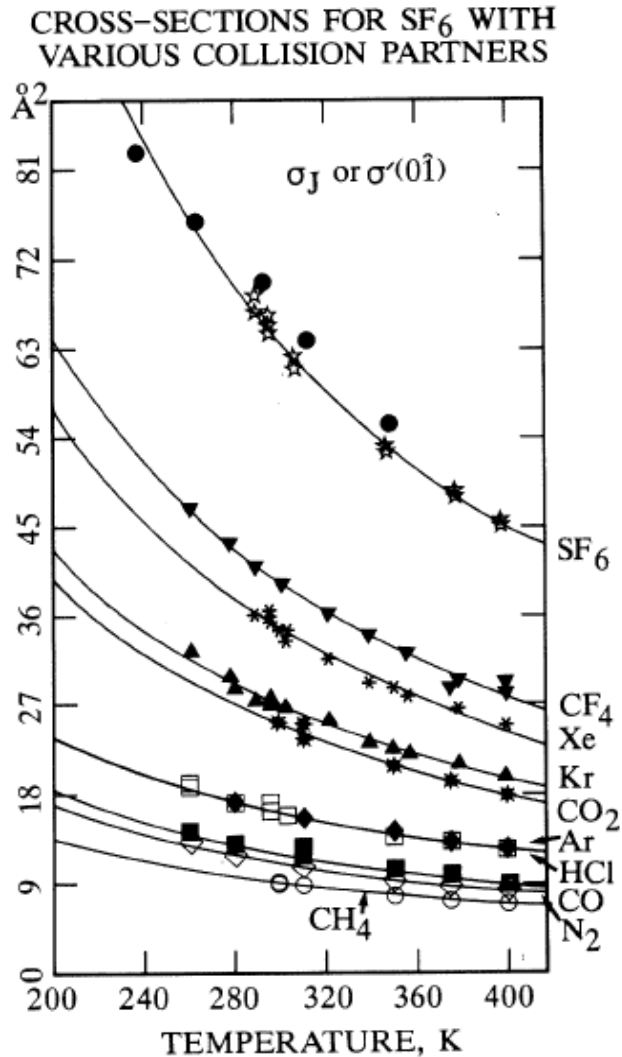


Angular momentum relaxation in binary collisions. Spin relaxation in the gas phase



Cynthia J. Jameson
University of Illinois at Chicago

Outline

- **INTRODUCTION:** anisotropy of intermolecular forces; effective cross sections; NMR can be used to study very fast processes such as rotational energy transfer
- **EXPERIMENTAL RESULTS:** the experiment; density and temperature dependence of T_1 ; The cross sections σ_J
- **THE CONNECTION BETWEEN σ_J and $V(r,\theta)$**
- **GENERAL TRENDS IN σ_J :** Can we say something about angular momentum relaxation without doing scattering calculations? the magnitudes at 300 K: a very simple model; the temperature dependence
- **CONCLUSIONS**

introduction

The forces between molecules in sufficiently dense gases produce a number of experimentally detectable effects:

- deviations from ideal gas (pV/RT) behavior
- viscosity, thermal conductivity,
- sound absorption
- broadening and shifts of spectral lines
- nuclear spin relaxation
- density dependence of any molecular electronic property such as chemical shifts
- collision-induced spectra

When detailed connection between intermolecular forces and experiments can be made, the experimental results may be used to determine, refine or test intermolecular potentials

Each of these experiments has a connection with the molecular collision process

CLASSICAL PICTURE OF RELATIVE MOTION OF TWO MOLECULES

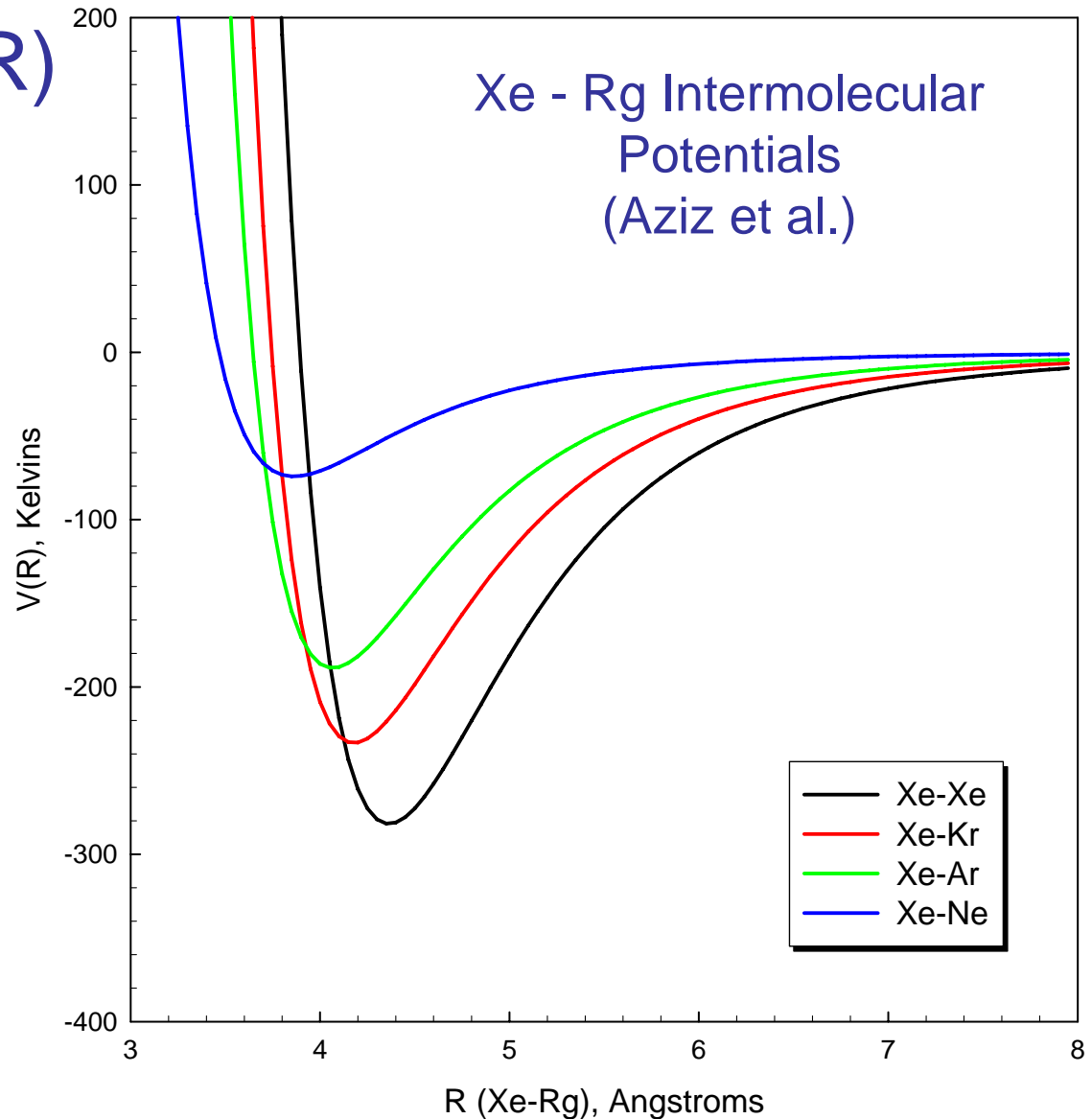
WITHOUT INTERMOLECULAR FORCES:



WITH INTERMOLECULAR FORCES:



The energy of interaction of two spherical molecules depends on the distance between the centers: $U(R)$

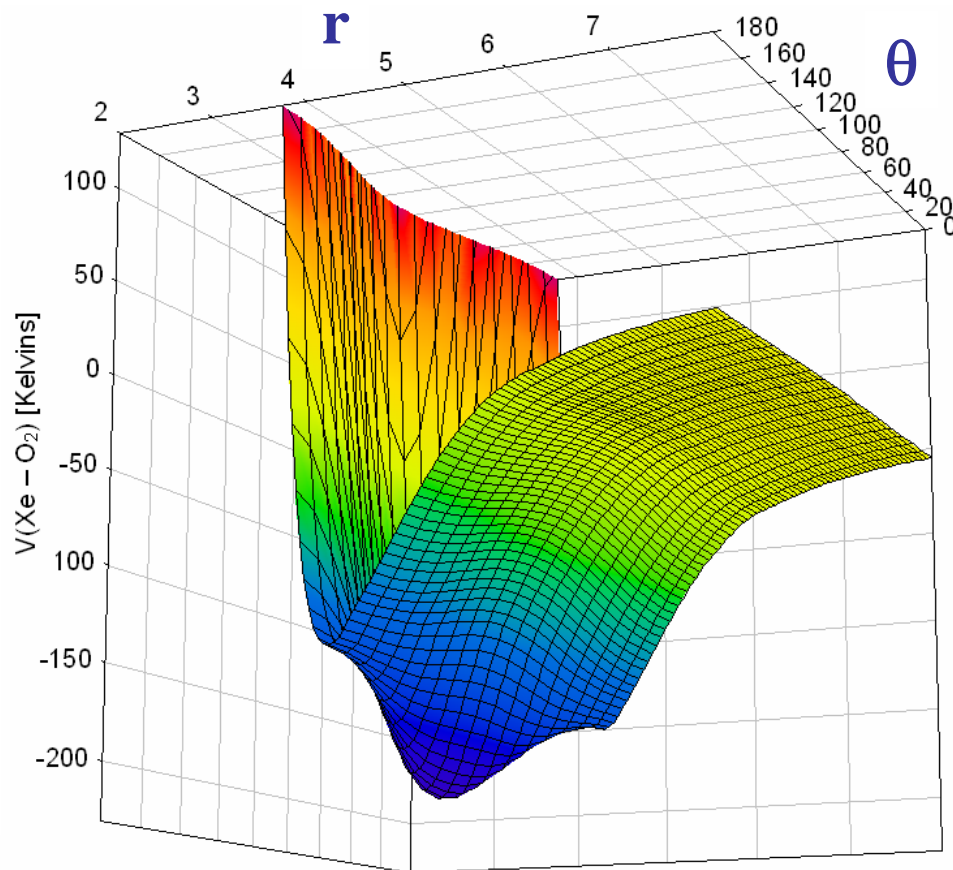


When one of the colliding pair of molecules is not an atom

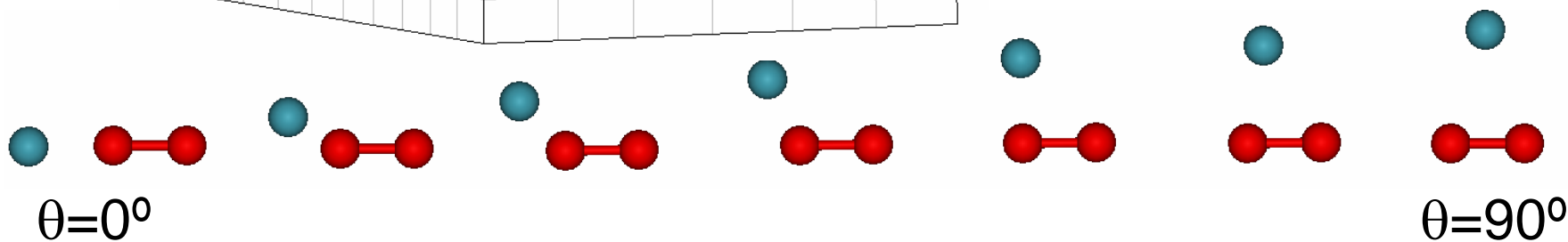
- the geometry of the problem is more complicated
- internal degrees of freedom (such as rotation and vibration) may become involved
- a molecule may have permanent electrical moments (dipole, quadrupole, octapole, hexadecapole, ...)

Thus, no longer isotropic $U(R)$

The energy of interaction of a spherical molecule with a linear molecule depends on the distance between the centers and the angle

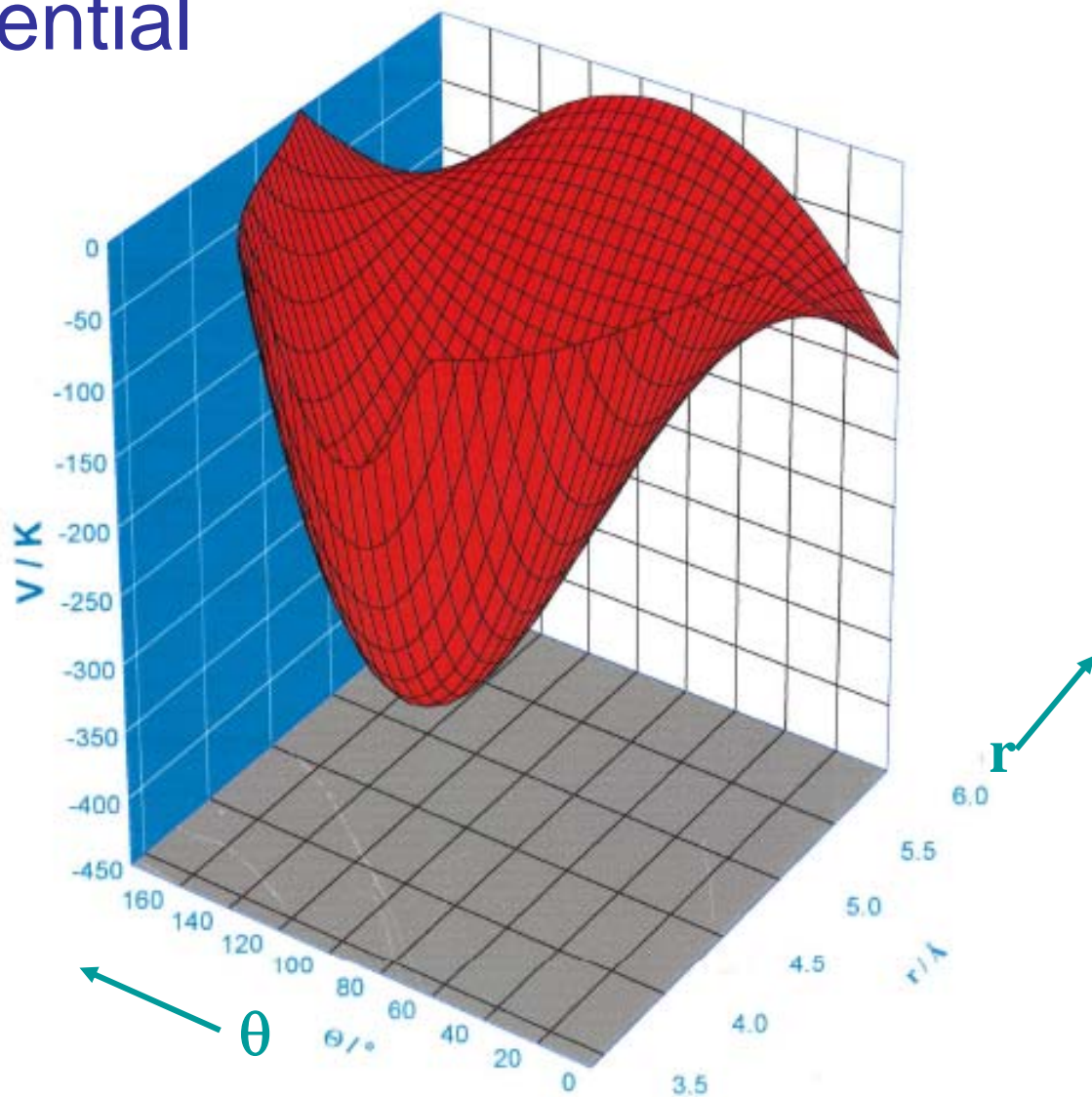


High quality potential function for Xe-O₂ from V. Aquilanti, D. Ascenzi, D. Cappelletti, M. de Castro, and F. Pirani, J. Chem. Phys. 109, 3898 (1998)



CO₂-Xe intermolecular potential

Buck Potential Surface for Xe - CO₂



The form of the anisotropy of intermolecular potentials is suggested by the form of the potential energy of interaction of two molecules in the **long-range limit**

$$U(R, \theta)_{\text{LONG-RANGE LIMIT}} =$$

$$-\frac{\alpha_2 \mu^2}{R^6} \left\{ 1 + \frac{9}{5} \frac{\mu}{R} P_1(\cos\theta) + \frac{1}{2} P_2(\cos\theta) + \frac{6}{5} \frac{\mu}{R} P_3(\cos\theta) \right\}$$

$$\frac{-3U_1 U_2 \alpha_1 \alpha_2}{(U_1 + U_2) R^6} \left\{ 1 + \frac{3}{5} R \left(\frac{A_{11}}{\alpha} + \frac{A_{12}}{\alpha} \right) P_1(\cos\theta) + \frac{\alpha_{11} - \alpha_{12}}{3\alpha_1} \frac{1}{2} P_2(\cos\theta) + \frac{1}{5} R \left(\frac{A_{11}}{\alpha} - \frac{4}{3} \frac{A_{12}}{\alpha} \right) P_3(\cos\theta) \right\}$$

$$P_1(\cos\theta) = \cos\theta \quad P_2(\cos\theta) = \frac{1}{2}(\cos^2\theta - 1) \quad P_3(\cos\theta) = \frac{1}{2} \left(\frac{5\cos^3\theta}{3} - 3\cos\theta \right)$$

For example,

$$U(R, \theta) = \epsilon \left\{ \frac{6}{n-6} x^{-n} - \frac{n}{n-6} x^{-6} \right\}$$

$$x = \frac{R}{R_{\min}(\theta)} \quad \epsilon = \sum_k \epsilon_k P_k(\cos\theta) \quad n(\theta)$$

For processes which occur in the gas phase which involve *binary collisions*, the **cross section** is a useful concept as a physical measure of the efficiency of the process.

these ***cross sections*** depend on the **isotropic potential** and to some extent its anisotropy:

from measurements of the viscosity,

$$\eta = \frac{kT}{\bar{v} \mathcal{S}(2000)}$$

bulk viscosity, κ ,

$$\kappa = \frac{k^2 T c_{int}}{\bar{v} c_v \mathcal{S}(0001)}$$

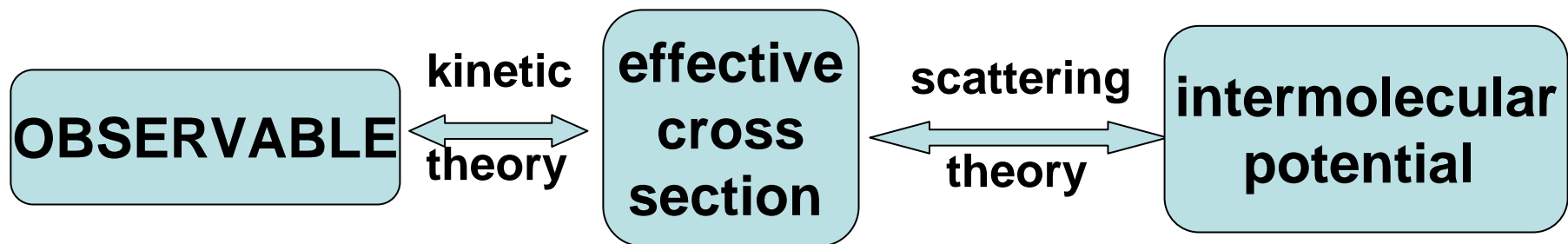
self-diffusion coefficient
of the gas,

$$D = \frac{kT}{\rho m \bar{v} \mathcal{S}(1000)}$$

thermal conductivity

$$\lambda = \frac{5k_B^2 T(1 + 2c_{int}/5k_B)}{8(\pi m k_B T)^{1/2} d^2 \mathcal{S}_T^*(10E)}$$

$$\mathcal{S}_T^*(10E) = \mathcal{S}_T(10E) / \pi d^2$$



crossed molecular beam		total differential cross sections
sound absorption	$\sigma(1001)$	TRANSPORT PROPERTIES
thermal conductivity	$\sigma(10E)$	
magnetic field on thermal conductivity	$\sigma(12q)$	
shear viscosity	$\sigma(20)$	
viscomagnetic effect	$\sigma(02\pi)$	
NMR spin relaxation spin rotation T_1^{SR}	σ_J	
NMR spin relaxation dipolar or T_1^Q quadrupolar	σ_θ	$\tau = (\rho \langle \mathbf{v} \rangle \sigma_\theta)^{-1}$ $(1/T_1)^Q_{lin} = [3(2I+3)/160 I^2(2I-1)] \omega_Q^2 \tau$
IRDR rotational relaxation	σ_{IRDR}	rotational relaxation rate constant $k = \langle \mathbf{v} \rangle \sigma$
rotational Raman	σ_{RR}	SPECTROSCOPY LINE SHAPES
resonant dipolar absorption	σ_{RA}	
nonresonant absorption	σ_{NRA}	
pressure broadening IR	σ_{PB}	
depolarized Raman	σ_{DPR}	
		lifetime or dephasing time $\tau = (\rho \langle \mathbf{v} \rangle \sigma)^{-1}$

some typical values

	$\omega_{\text{SR}}^2, \text{ s}^{-2}$	$\langle \mathbf{J}^2 \rangle_{300\text{K}}$	$\tau_{300\text{K}}, \text{ s}$	$T_1^{\text{SR}}_{300\text{K}}$ 10 amagat
$^{15}\text{N}^{15}\text{NO}$	6.1×10^6	1069	5×10^{-10}	1.0 s
$^{13}\text{CH}_4$	2.6×10^8	60	1×10^{-8}	10.2 ms
C^{19}F_4	4.8×10^7	1645	1×10^{-9}	19.5 ms
^{13}CO	1.1×10^9	108	1×10^{-9}	12.3 ms



FAST
dynamic
processes

rotational relaxation
& molecular reorientation



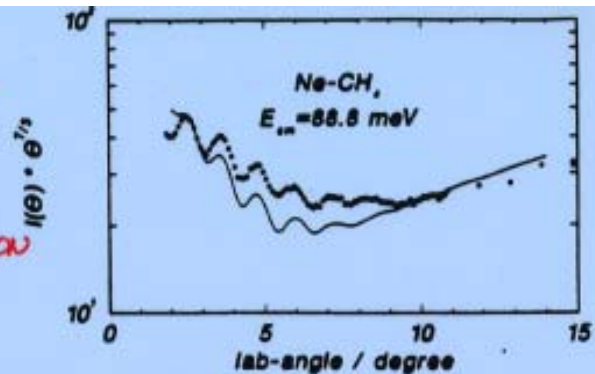
SLOW
NMR
time
scale

Comparison of experimental effective cross sections for N_2-N_2

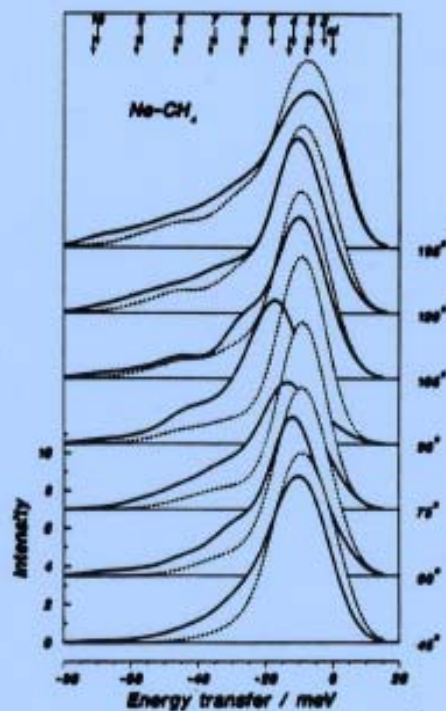
Experiment	Dominant dynamic variable	Cross section ^a	Room T value (\AA^2)
Sound absorption	J^2 change	$\sigma(0001)$ or σ_{rot}	7.6 ± 0.8 10.4
Viscosity	$W W'$	$\sigma(20)$	35.0 ± 0.4
Viscomagnetic effect	$J J'$ tensor polarization	$\sigma(02\pi)$	23.7 ± 0.9
Depolarized Rayleigh	$J J'$ tensor polarization	$\sigma(0\hat{2})^b$ or $\sigma(\text{DPR})$	$34.4 \pm 0.6, 35.5$
NMR relaxation (quadrupolar)	$J J'$ tensor polarization ^c	$\sigma'(0\hat{2})$ or σ_{θ}	29.7
NMR relaxation (spin rotation)	J vector polarization ^c	$\sigma'(0\hat{1})$ or $\sigma_r(\text{SR})$	14.9 ± 0.4
Magnetic effect on heat conductivity	$W J J'$ polarization	$\sigma(12q)$	43

crossed molecular beams

CROSSED
MOLECULAR
BEAMS
PROVIDE
THE MOST
DETAILED
INFORMATION



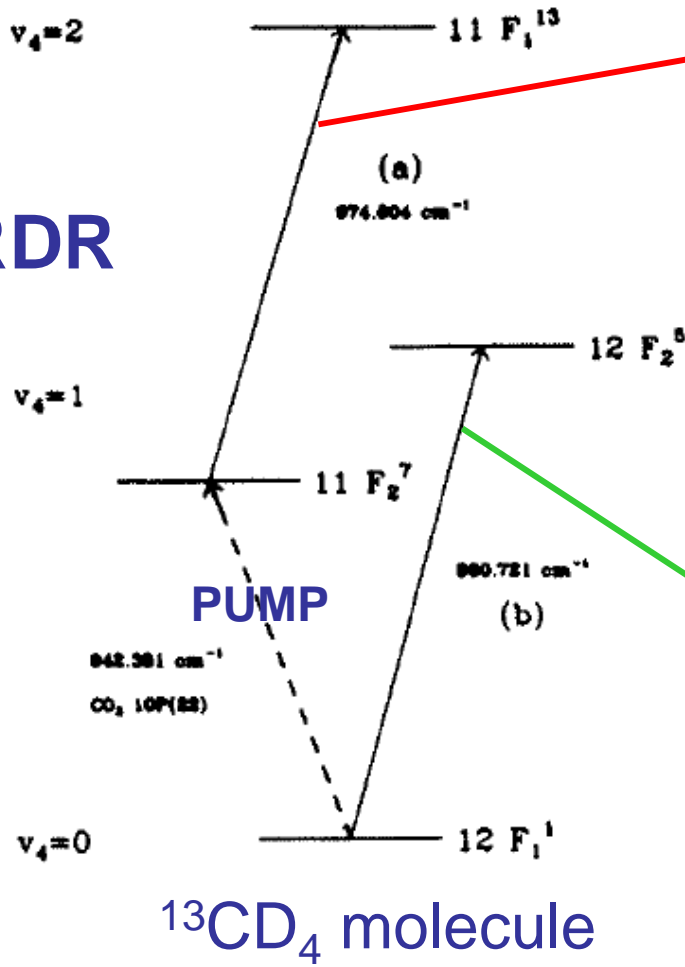
Measured and calculated total differential cross sections



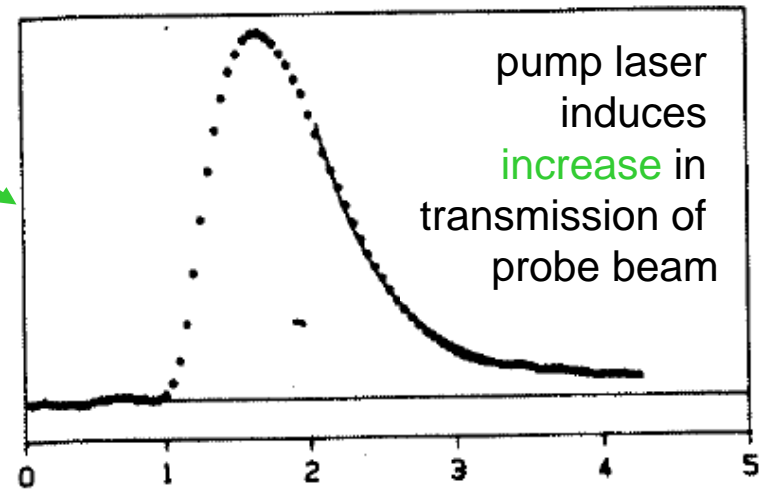
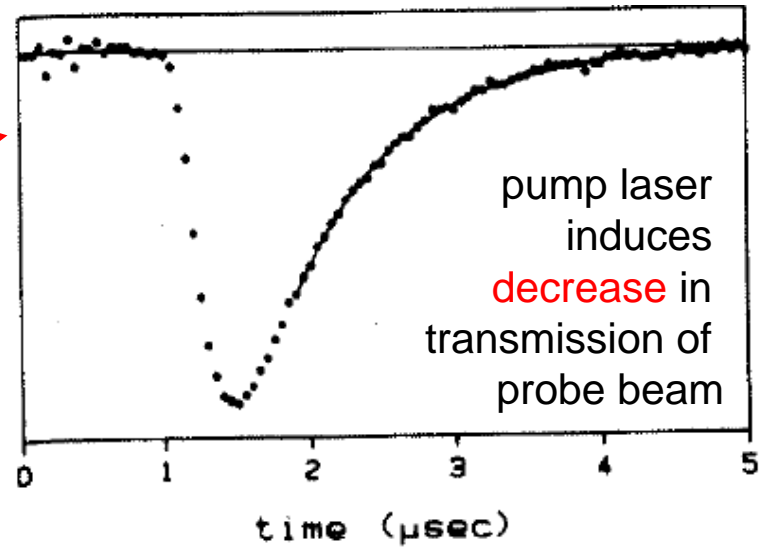
BULL, SCOLES + co-workers

infra-red double resonance provides state-to-state rotational relaxation

IRDR



decay curves of the IRDR signal



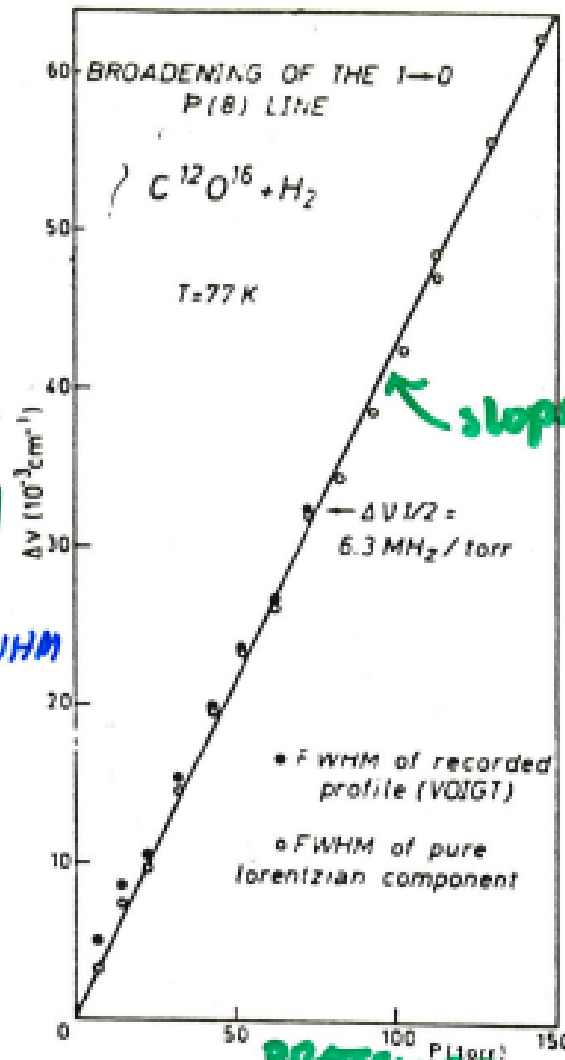
τ obtained from exponential fit

FIG. 2. Pump-probe scheme for rotational-state depopulation measurements by three-level double resonance.

Steinfeld and coworkers

pressure-broadening of infra-red

↑
HALF
WIDTH
($\Delta\nu$)
FWHM



↖ slope = broadening coefficient γ

Pressure →

FIG. 4. $\Delta\nu$ vs pressure in the case of P(8) line for C¹²O¹⁶ diluted in H₂ at 77 K.

SO DOES PRESSURE-BROADENING OF INFRARED LINES PROVIDE STATE-LABELED DATA.

nuclear spin relaxation

- rf field is used to disturb nuclear spins from thermal equilibrium in an external static magnetic field
- recovery of magnetization in the direction of the external static field is characterized by a time constant T_1 (spin lattice relaxation time)

Classical picture:




- INTRAmolecular magnetic field is generated by rotation of the molecule. Molecular rotation frequencies are in the microwave region. The only effective frequencies which affect nuclear spins are in the rf region. Therefore, only a **MODULATION** of the intramolecular magnetic fields by **INTERMOLECULAR COLLISIONS** can contribute to spin relaxation.

connection between T_1 and anisotropy (angle dependence) of intermolecular potential

- The strongest magnetic interactions which couple NUCLEAR SPINS to the other degrees of freedom (rotation) are a function of molecular orientation and rotational angular momentum
- In dilute molecular gases these intramolecular interactions:
 - intramolecular dipole-dipole interaction
 - spin rotation interaction
 - quadrupolar interaction for nuclei with spin $> \frac{1}{2}$

are made time-dependent by collisions which either reorient a molecule or change its rotational angular momentum – only anisotropic intermolecular interactions can give rise to the requisite TORQUES

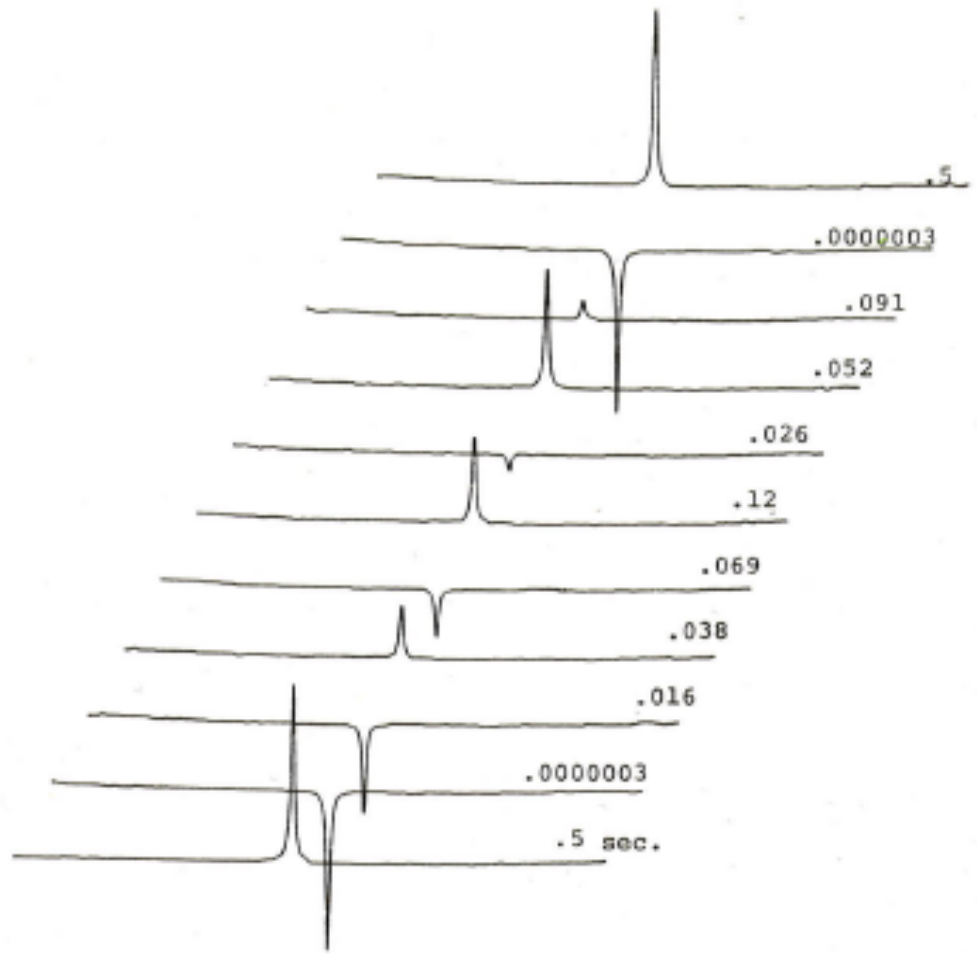
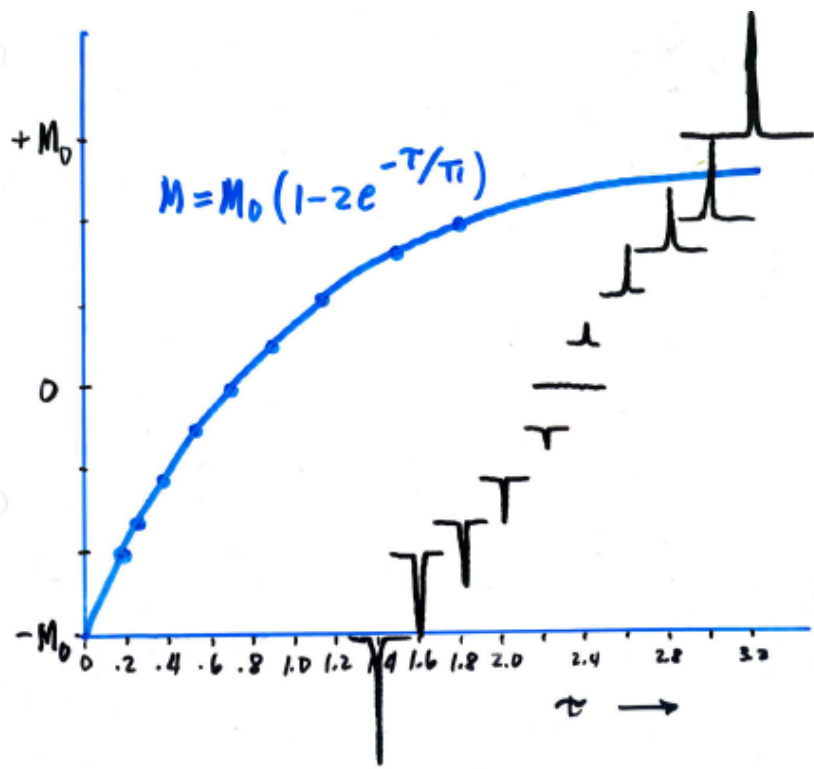
the spin relaxation experiment

- Start with nuclear spins in thermal equilibrium. Magnitude of the equilibrium magnetization M_0 along the direction of external magnetic field can be observed in an nmr experiment as 
- If we subject the spins to an rf pulse which tips the magnetization 180° , then immediately observe (i.e., no delay) 
- We can wait a time t after the 180° deg pulse before observing the magnetization:
- The observed intensity of the peak depends on the extent to which the nuclear spin system has recovered from $-M_0$ towards the thermal equilibrium $+M_0$. 

By doing several experiments, starting out always at thermal equilibrium: **invert** with a 180° pulse, **wait** t seconds, **observe**, we can find the time constant T_1 characteristic of the nuclear spin system. This sequence of events known as an **inversion recovery experiment**, can automatically be carried out in a simple program.

The magnetization for a time delay t is given by

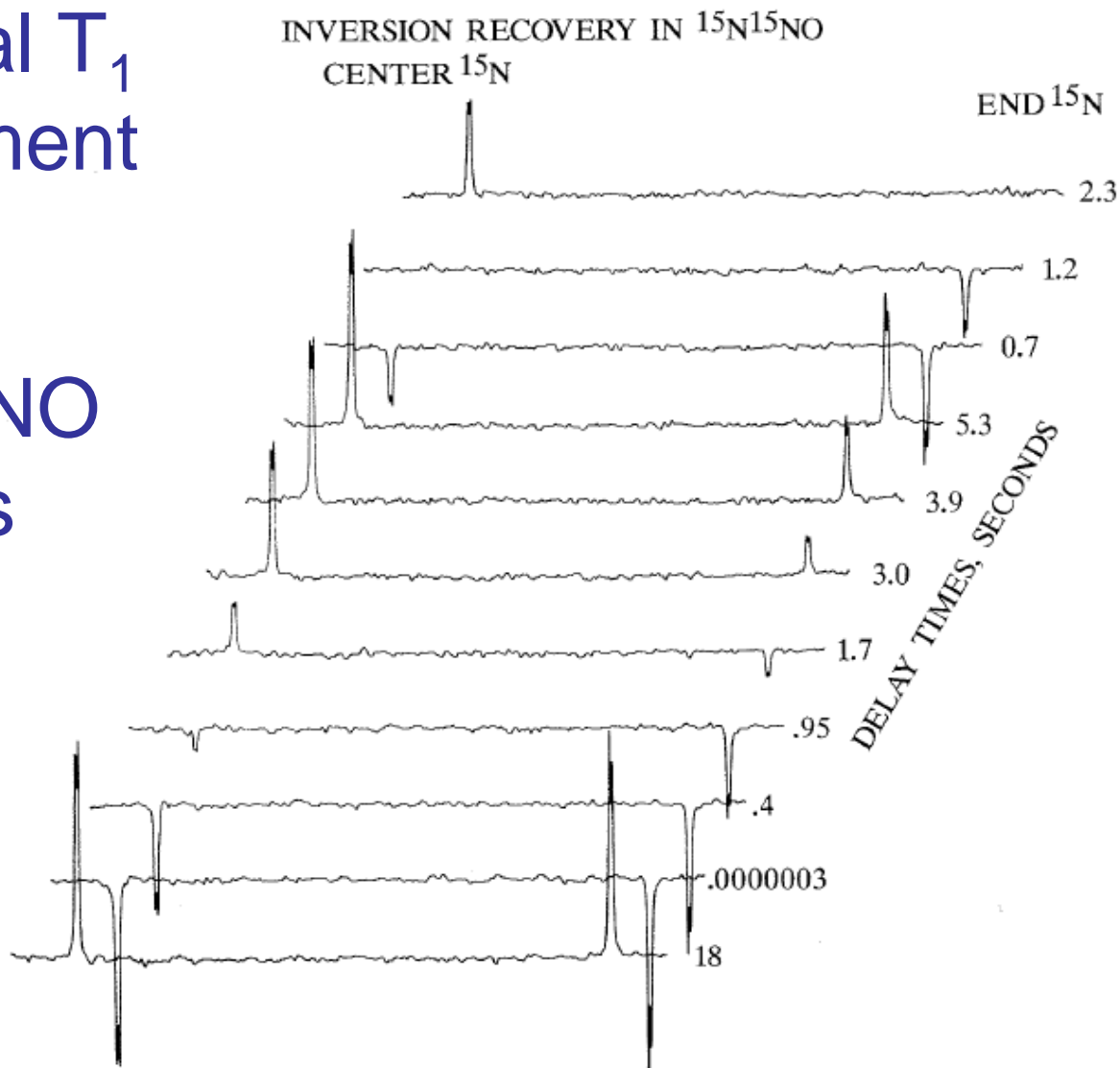
$$M = M_0[1 - 2\exp(-t/T_1)]$$



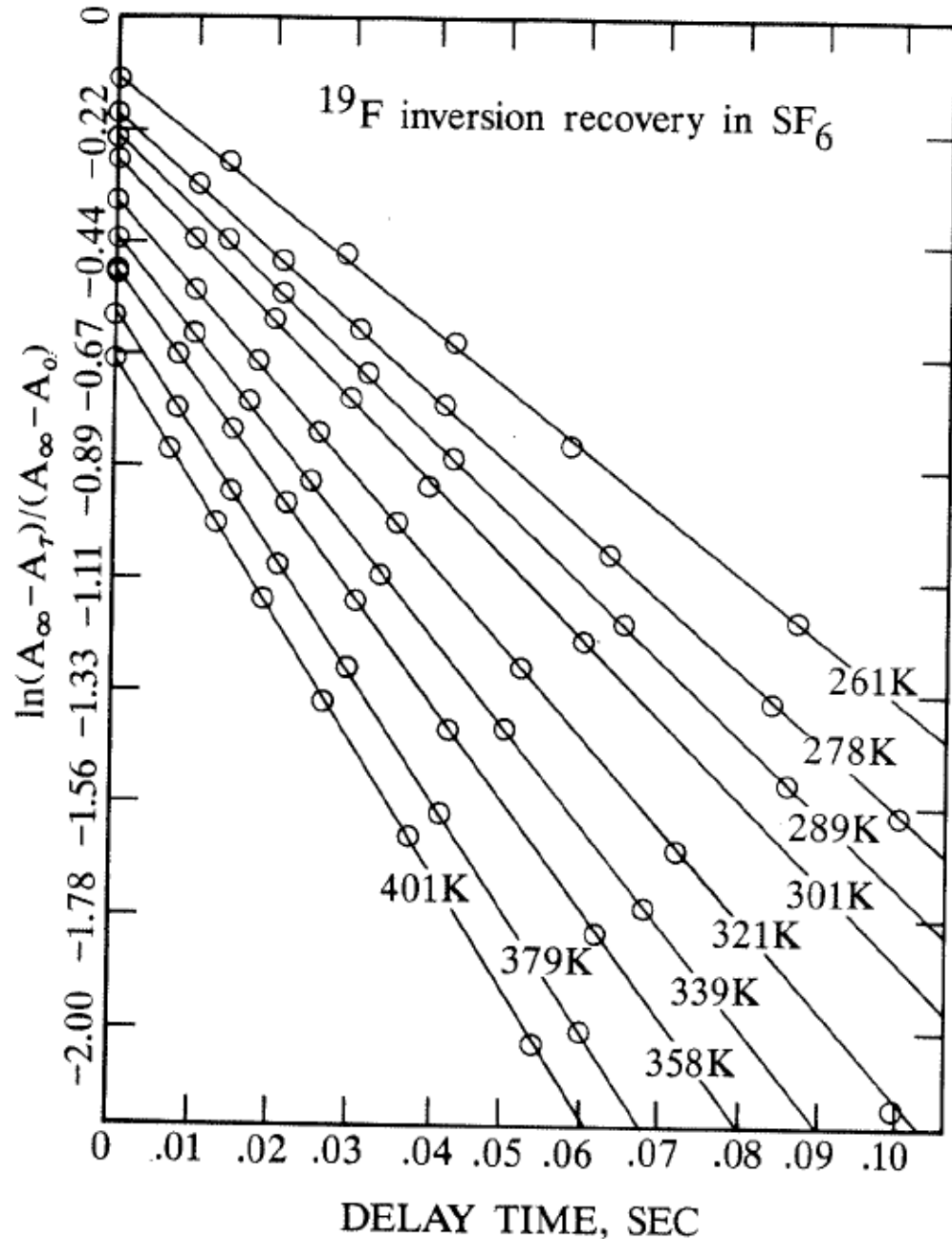
Pure N_2
 Numbers on right are delay times

a typical T_1
experiment

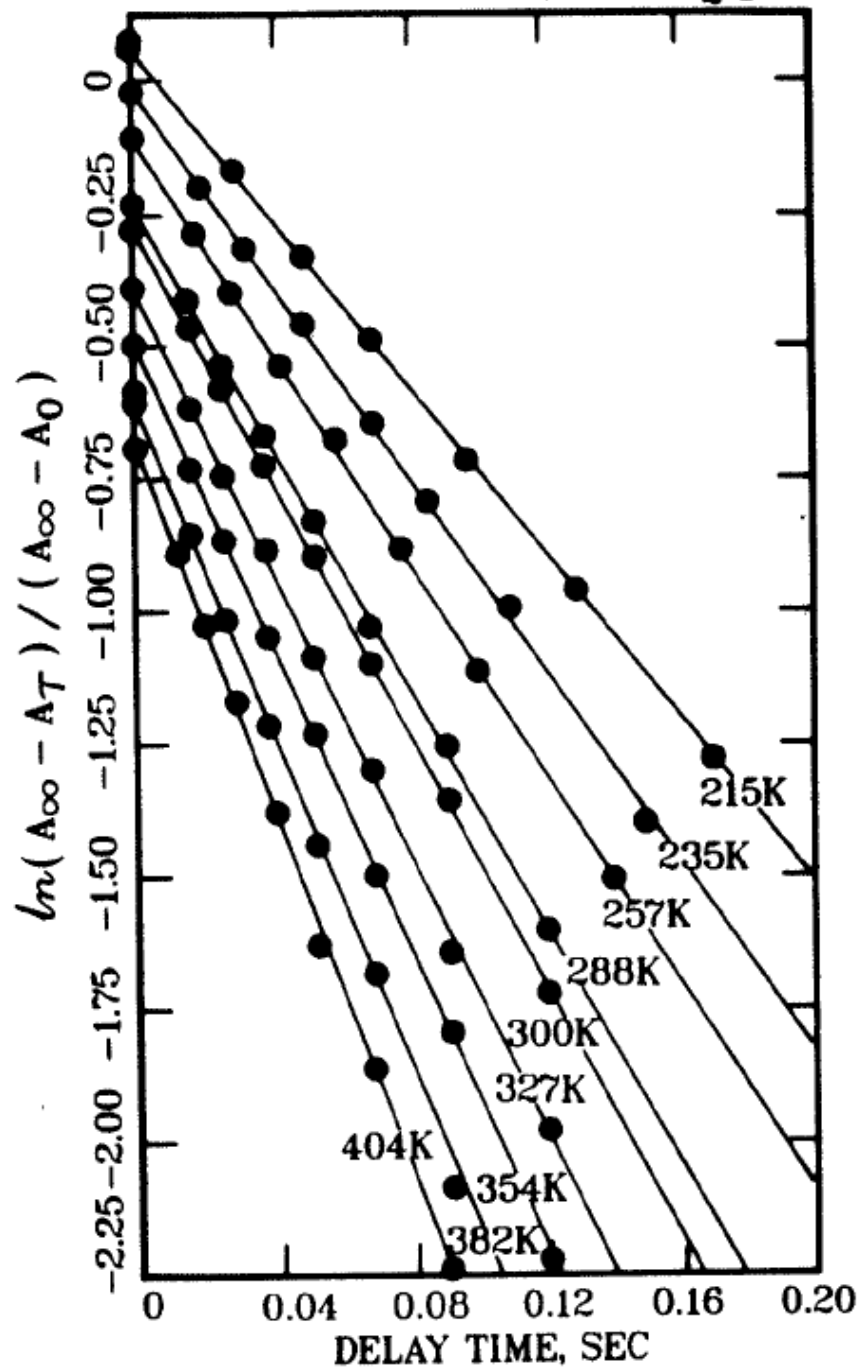
$^{15}\text{N}^{15}\text{NO}$
gas



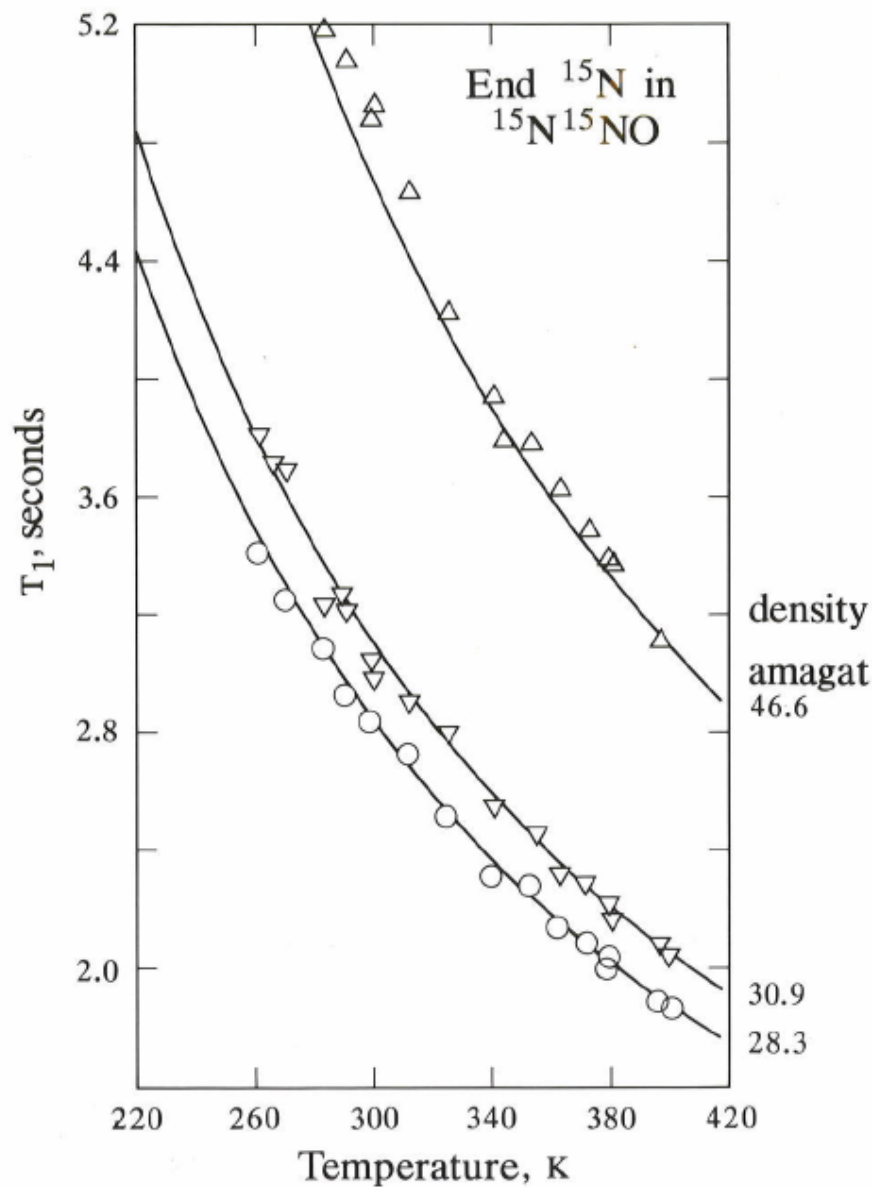
typical
data for a
sample at
different
temperatures



^{15}N inversion recovery in $^{15}\text{N}_2$ gas

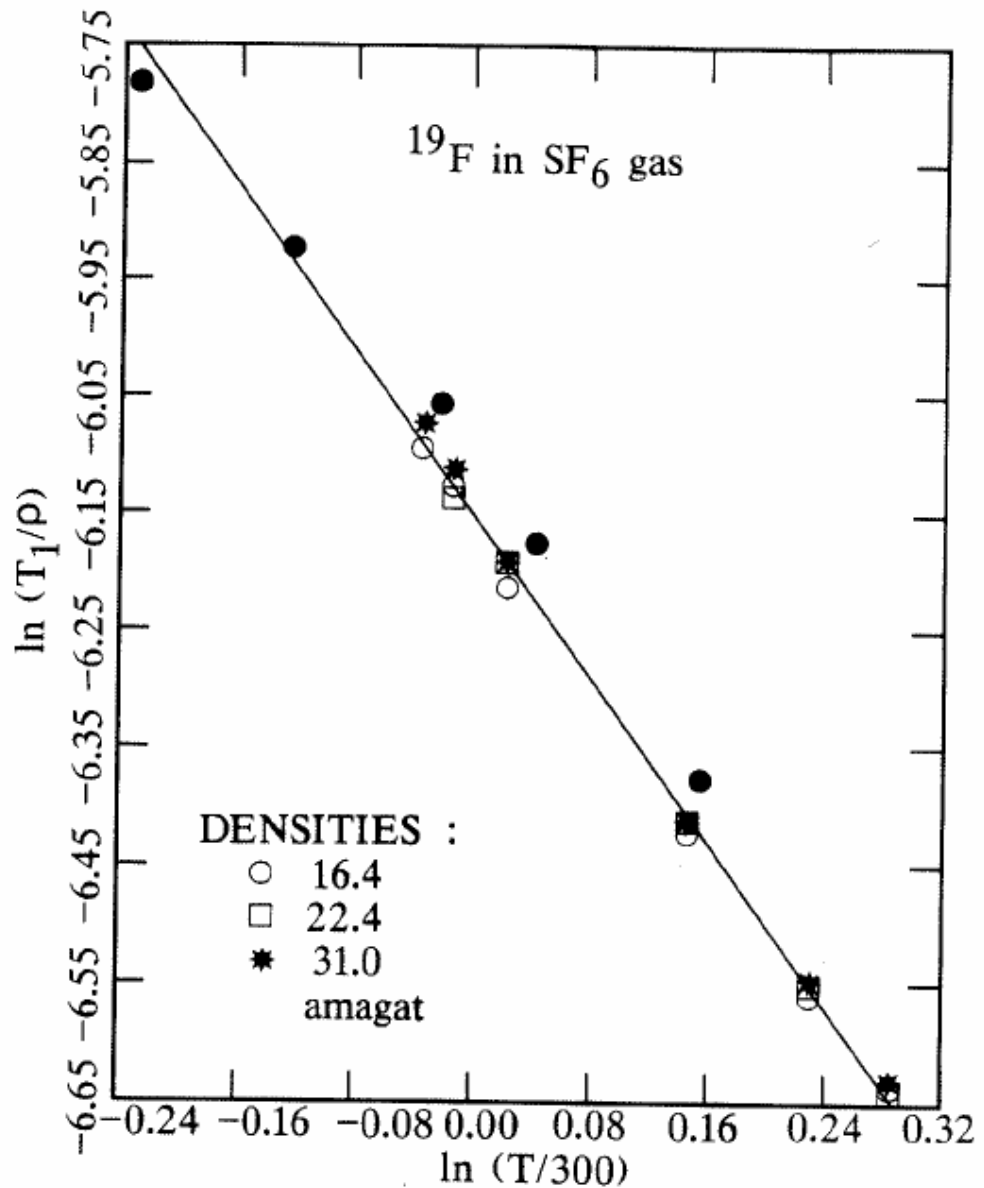


typical T_1
dependence
on density and
temperature

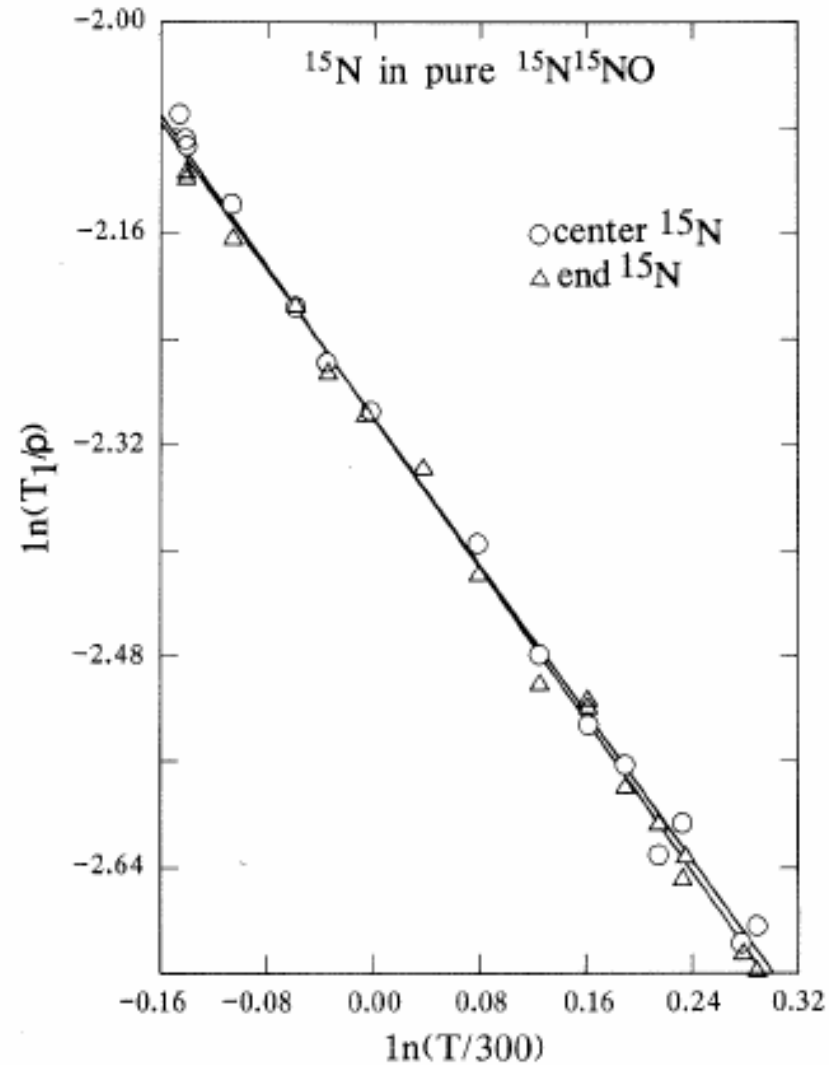


Linear dependence on density makes T_1/ρ a characteristic quantity

● other lab



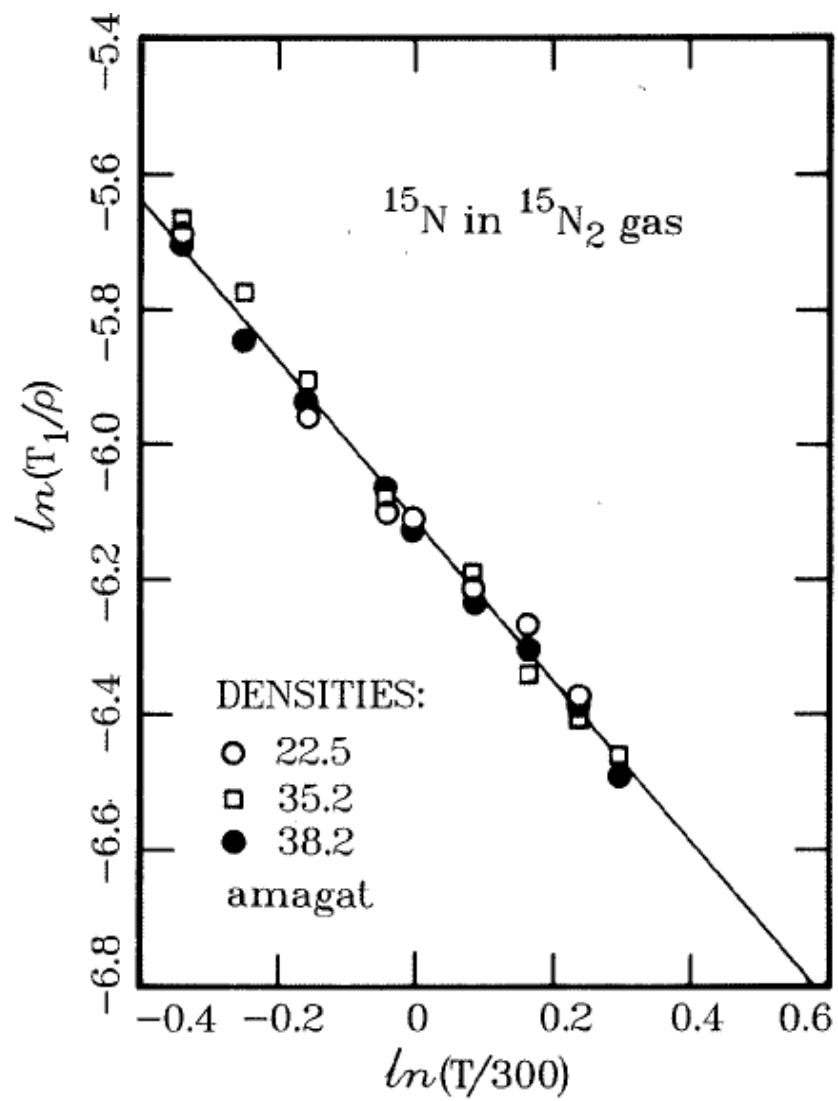
we find a
power law
dependence
on
temperature



temperature dependence of T_1/ρ

$$(T_1/\rho) = (T_1/\rho)_{300\text{K}}(T/300)^{-m}$$

where m is not an integer, often close to 1



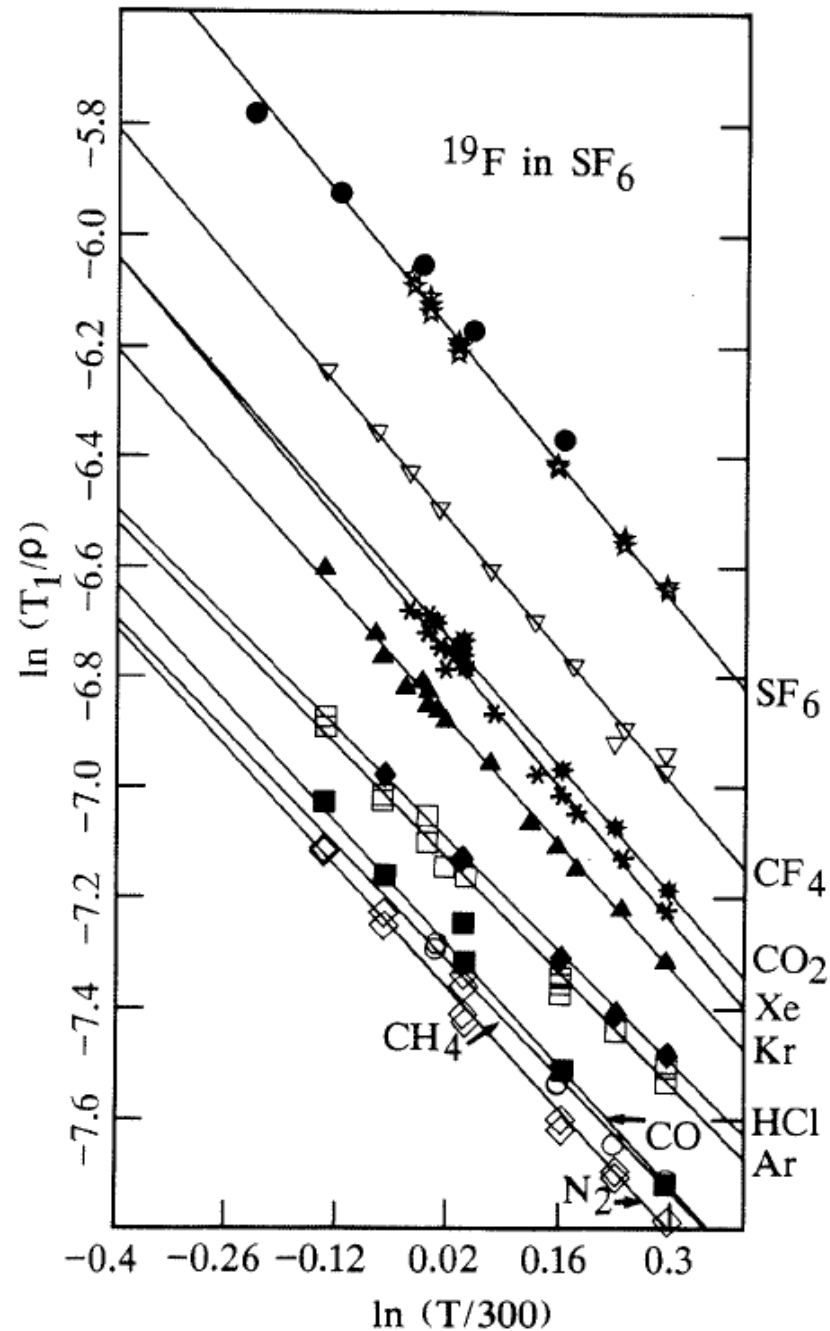
for molecule X in a buffer gas A

Relaxation by the spin-rotation mechanism is caused by X-X collisions and by X-A collisions. In this study it is **empirically established** that these effects are additive in the density range 5-50 amagat, i.e.,

$$T_1 = \rho_X (T_1/\rho)_{X-X} + \rho_A (T_1/\rho)_{X-A}$$

T_1/ρ
for various
collision
partners

● other lab



cross sections for rotational angular momentum transfer

classical

$$\sigma_J(T) = (1/2\langle J^2 \rangle^T) \int_0^\infty \langle (\Delta \mathbf{J})^2 \rangle 2\pi b db,$$

where $\Delta \mathbf{J}$ is the change in the rotational angular momentum vector of the molecule by a collision

$$\sigma_J = \frac{1}{2\langle J^2 \rangle} \int_0^\infty 2\pi b db \langle [\mathbf{J}(1) - \mathbf{J}(0)]^2 \rangle,$$

where $\mathbf{J}(0)$ and $\mathbf{J}(1)$ are the rotational angular momentum vectors before and after a collision

the average $\langle \rangle$ denotes the average over the initial distribution of internal states before a collision and the initial distribution of relative velocities.

semiclassical

$$\sigma_J = [\mathbf{d} \cdot (\boldsymbol{\sigma})^{-1} \cdot \mathbf{P} \cdot \mathbf{d}]^{-1}.$$

The weighting factors are determined by the populations of the rotational states in \mathbf{P} and the initial rotational quantum numbers J_i (before collision) in \mathbf{d} whose elements d_i are given by

$$d_i = [J_i(J_i + 1) / \langle J(J + 1) \rangle]^{1/2}.$$

$\langle J(J + 1) \rangle$ is the equilibrium thermal average square of the rotational angular momentum.

$\boldsymbol{\sigma}$ is the scattering matrix for the J vector, with elements

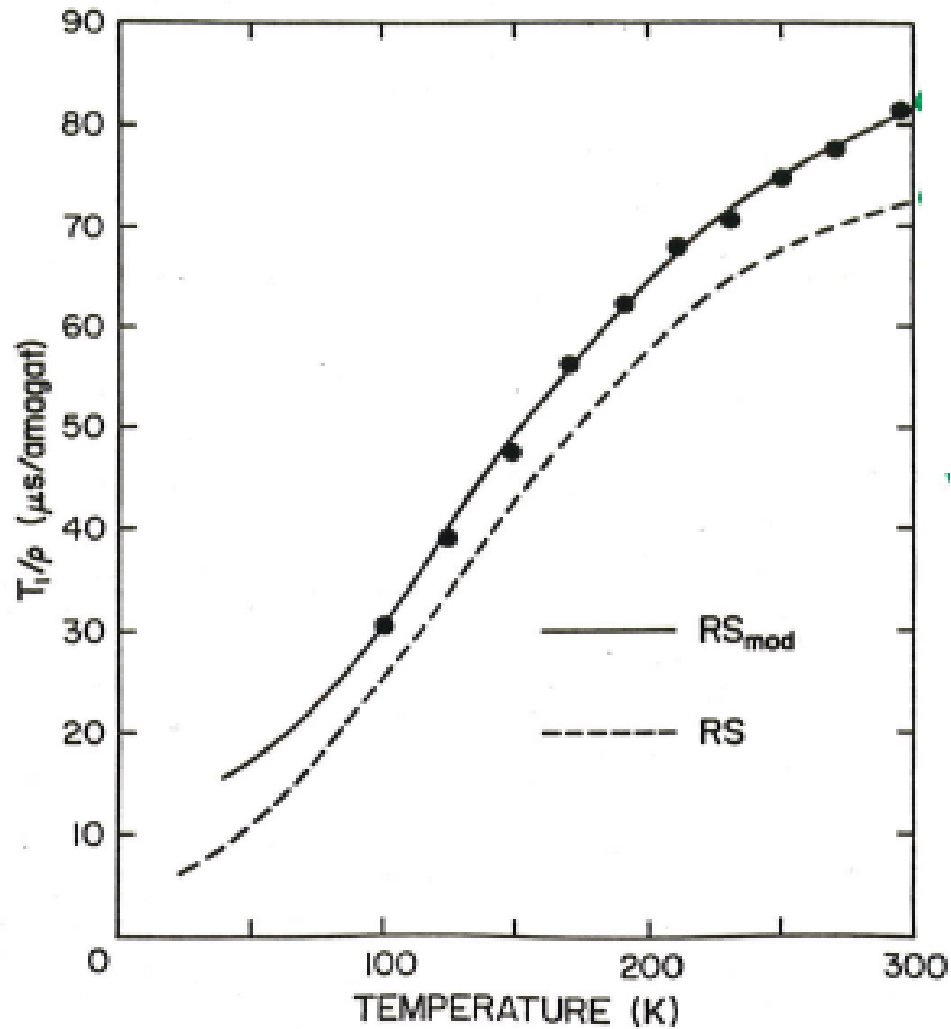
$$\sigma_{fi} = \frac{1}{v} \int_0^\infty 2\pi b db \langle v(\delta_{fi} - \mathcal{P}_{fi} \cos \alpha) \rangle$$

involving \mathcal{P}_{fi} , the probability that a collision changes the energy from the quantum level i to f , α the angle between \mathbf{J}_i and \mathbf{J}_f . These collision-induced transitions arise only from the angle-dependent terms in the intermolecular potential energy.

Nielsen + Gordon

QUANTUM - MECHANICAL

$\frac{T_1}{\rho_{Ne}}$



slightly
modified
Scoles potential

McCourt and Armstrong

relation between spin-rotation T_1 and cross section σ_J

Cross sections for rotational angular momentum transfer σ_J , were found by using Gordon's theory²³:

$$\left(\frac{T_1}{\rho}\right) = \frac{3\bar{v}}{2(J(J+1))C_1^2} \sigma_J(T)$$

C_1^2 \leftarrow C_{eff}^2

$$= \frac{3B_0}{2kT C_1^2} \left(\frac{8kT}{\pi\mu}\right)^{1/2} \sigma_J(T). \quad (4)$$

FOR LINEAR MOLECULES

FOR SPHERICAL TOPS

B_0 is the rotational constant and C_1 is the spin rotation con-

relation between quadrupolar T_1 and cross section $\sigma_{\theta,2}$

$$(T_1^Q)^{-1} = \frac{3}{40} \frac{(2I+3)}{I^2(2I-1)} \left(\frac{e^2 q Q}{\hbar} \right)^2 \left\langle \frac{j^2}{4j^2-3} \right\rangle \frac{1}{\rho \langle v \rangle \sigma_{\theta,2}}$$

$$\left\langle \frac{j^2}{4j^2-3} \right\rangle = \langle J(J+1)/(2J-1)(2J+3) \rangle$$

approaches the limiting value 1/5 **for spherical tops**
except at extremely low T

For spherical top probe molecules:

$$T_1^Q = \frac{200}{3} \frac{I^2(2I-1)}{(2I+3)} \left(\frac{\hbar}{e^2 q Q} \right)^2 \rho \langle v \rangle \sigma_{\theta,2}$$

relation between quadrupolar T_1 and cross section $\sigma_{\theta,2}$

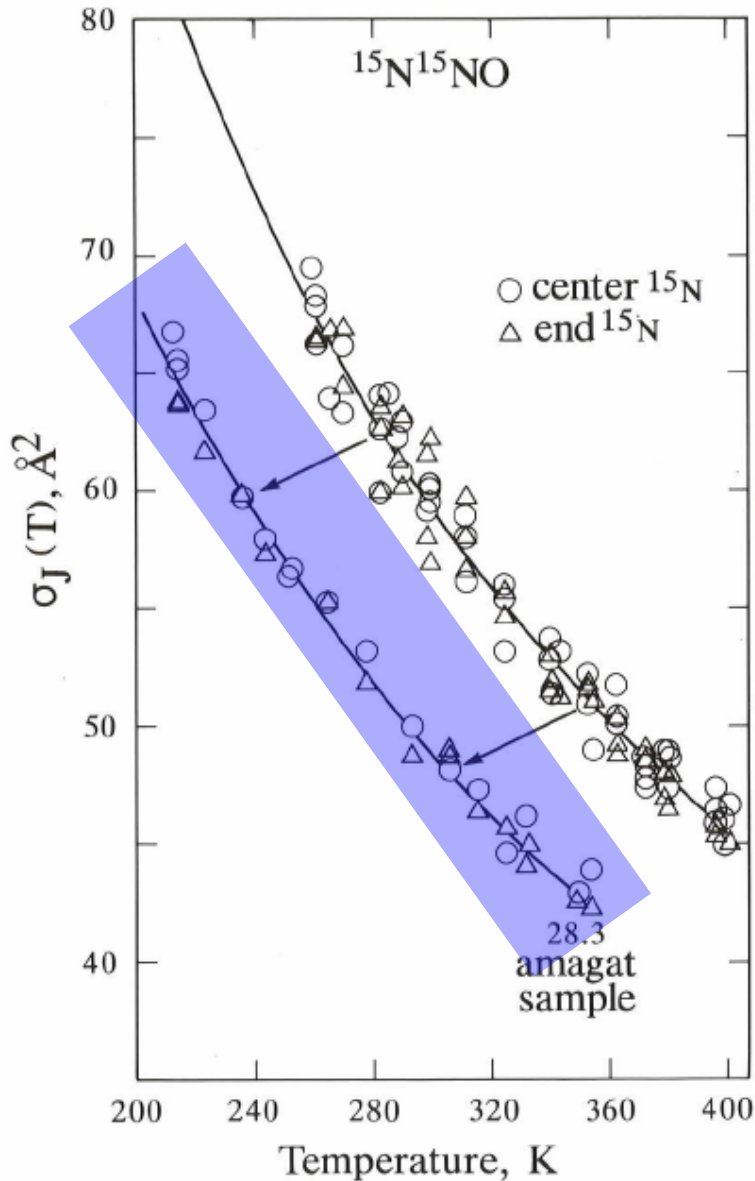
$\left\langle \frac{j^2}{4j^2 - 3} \right\rangle$ approaches the limiting value 1/4

for linear molecules, except at extremely low T

For linear probe molecules:

$$\left(\frac{T_{1Q}}{\rho} \right)_{\text{lin}} = \frac{160I^2(2I-1)}{3(2I+3)} \left(\frac{\hbar}{eqQ} \right)^2 \bar{\nu} \sigma_{\theta,2}$$

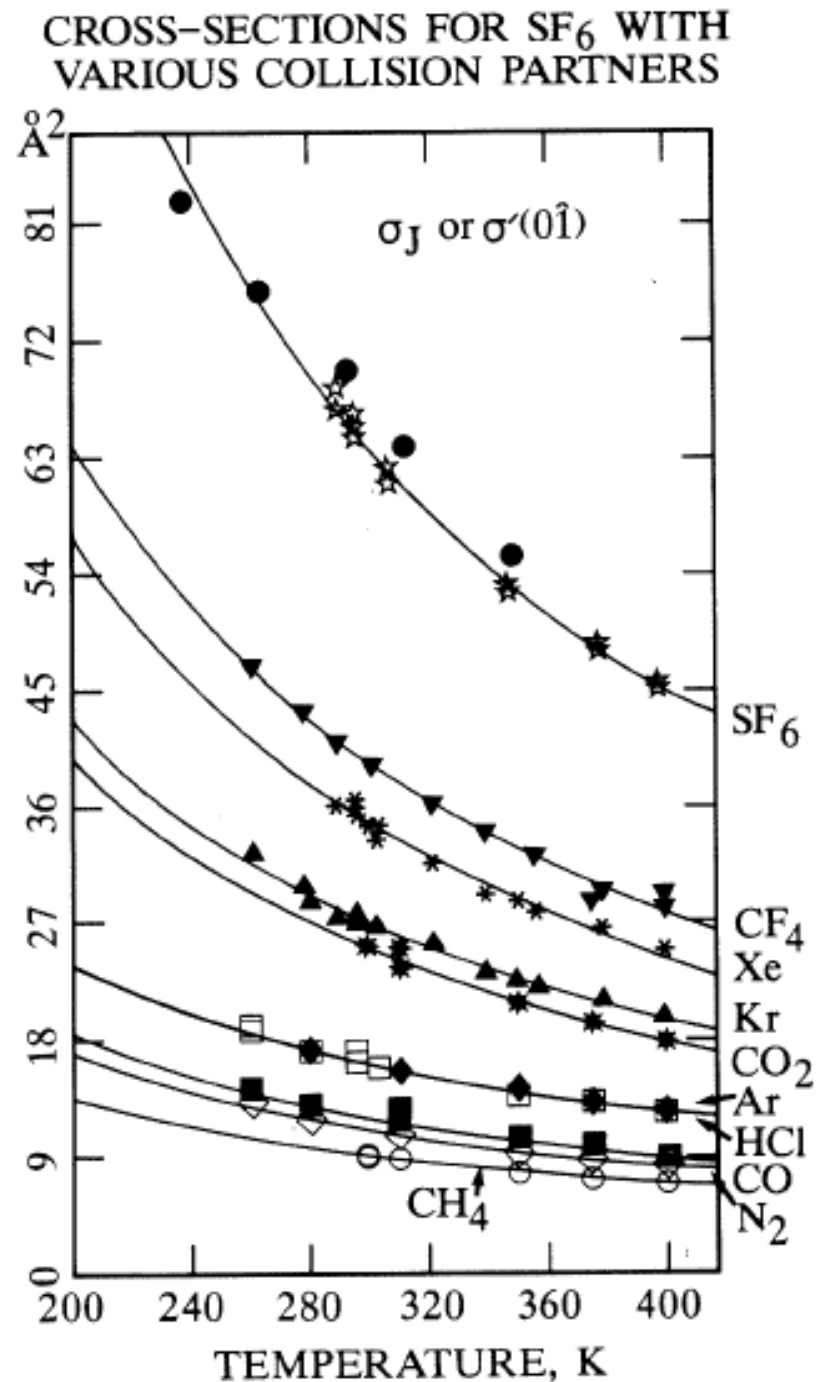
all nuclei
in the same
molecule
provide
the same
cross section



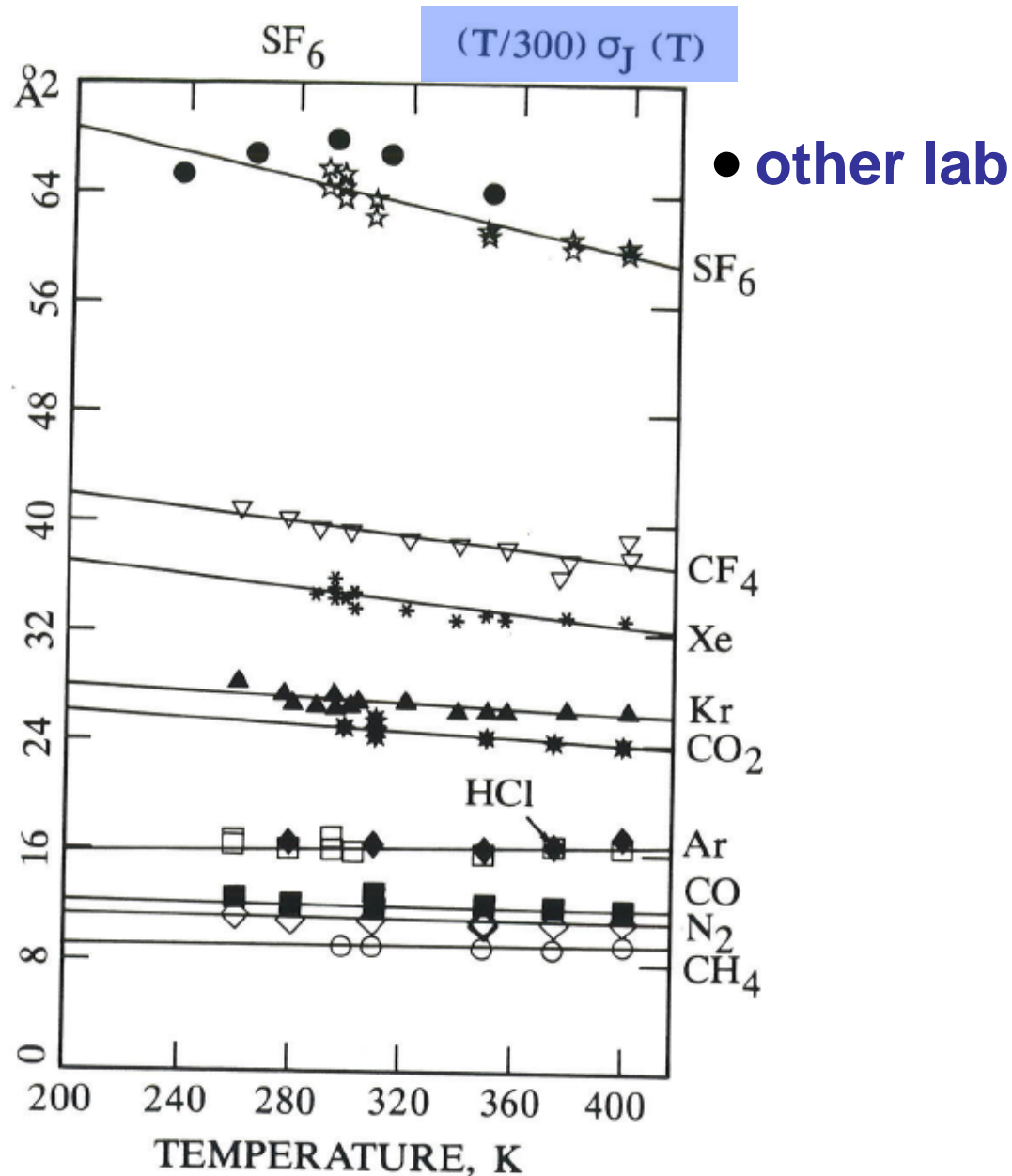
(data for one sample is displaced to show that center and end nuclei provide the same cross section)

cross sections for SF₆ with various collision partners

● other lab



cross section
depends
on T^{-m}
where $m \neq 1$



probe molecules and nuclei

Spin = $\frac{1}{2}$

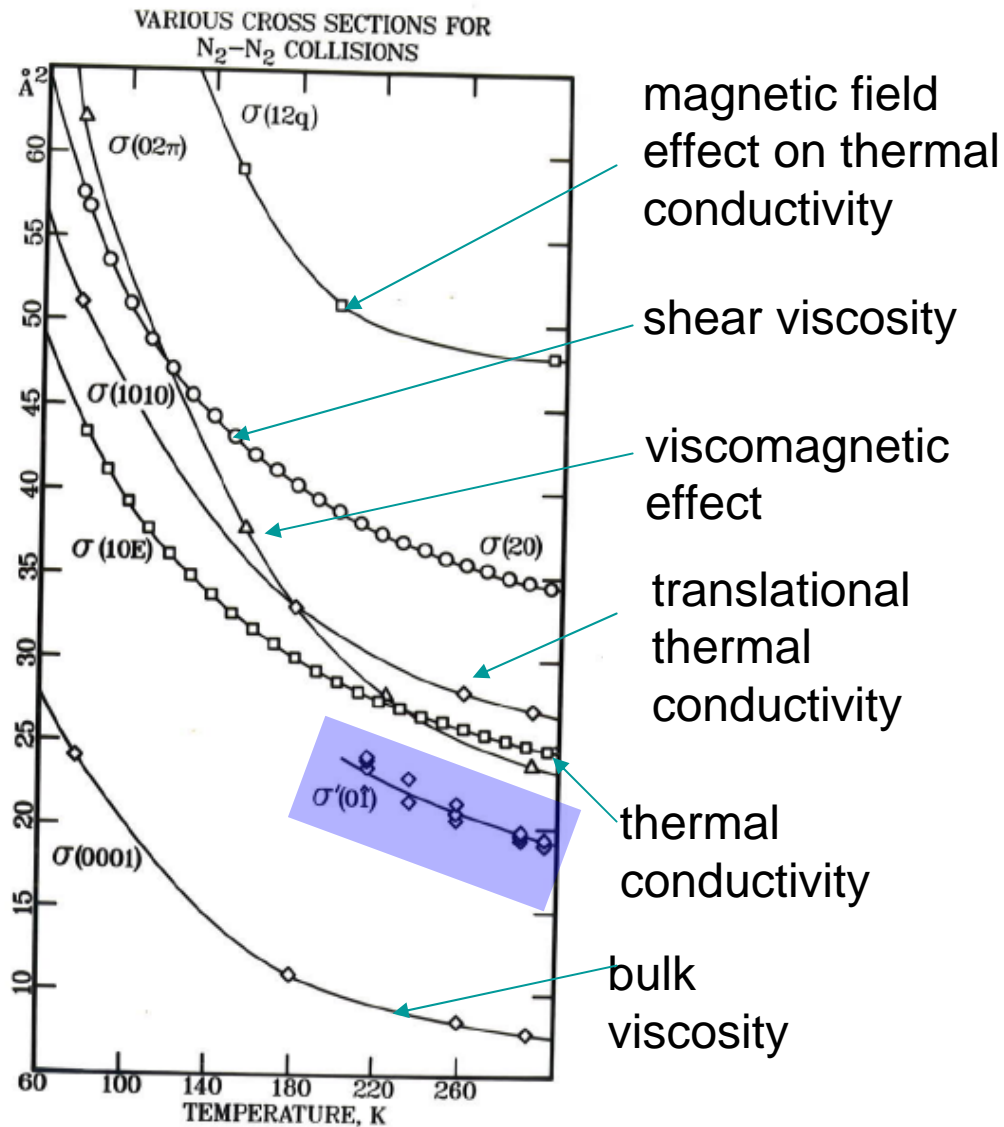
- ^{19}F in CF_4 , SF_6 , SeF_6 , TeF_6
- ^{13}C in CO , CO_2 , CH_4
- ^{15}N in N_2 , $^{15}\text{N}^{15}\text{NO}$

Spin $> \frac{1}{2}$

- ^{14}N in N_2 , $^{14}\text{N}^{14}\text{NO}$
- ^2D in CD_4

Buffer gases: CH_4 , N_2 , CO , Ar , HCl , CO_2 , Kr , CH_4 , Xe ,
 SF_6 , SeF_6 , TeF_6

Various N_2-N_2 cross sections compared with cross section σ_J aka $\sigma'(01)$ from spin-rotation relaxation data



how are the cross sections to be evaluated from intermolecular potentials?

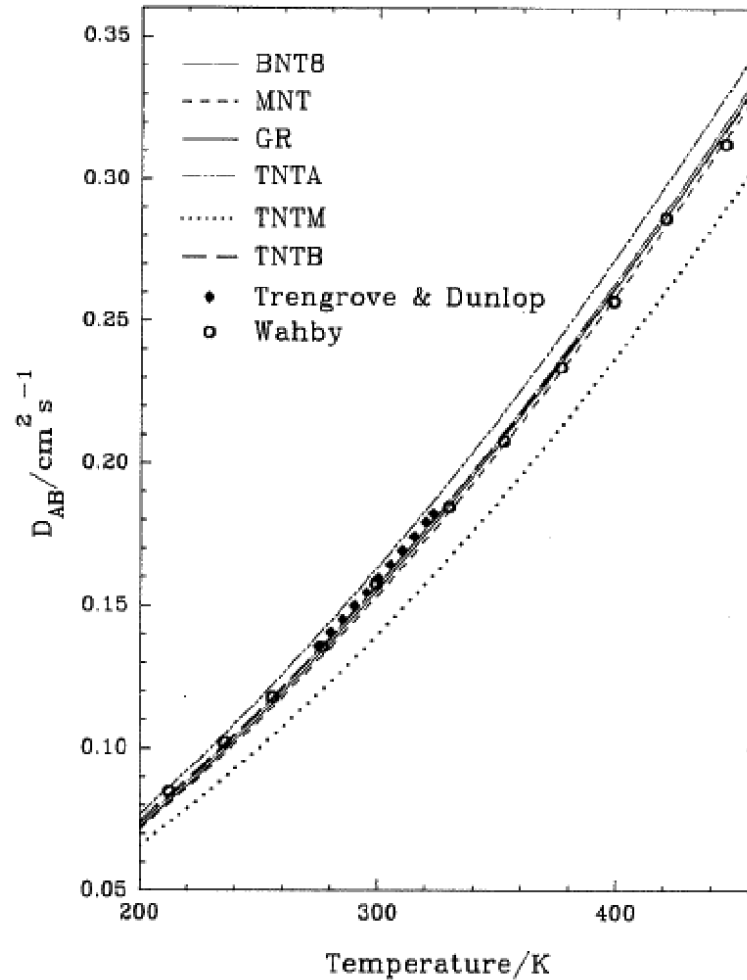
- Must be able to determine **trajectories** of molecular collisions.
- From the collision trajectories the rotational angular momentum **before ($\mathbf{J}(0)$)** and **after ($\mathbf{J}(1)$)** collision may be compared, $[\mathbf{J}(1) - \mathbf{J}(0)]$
- The other initial conditions: relative velocity, orientation, and impact parameter b are chosen according to some convenient sampling scheme which distributes these parameters uniformly over the appropriate distributions.
- The calculation is repeated a sufficient number of times to average over the initial conditions.

classical trajectory calculations

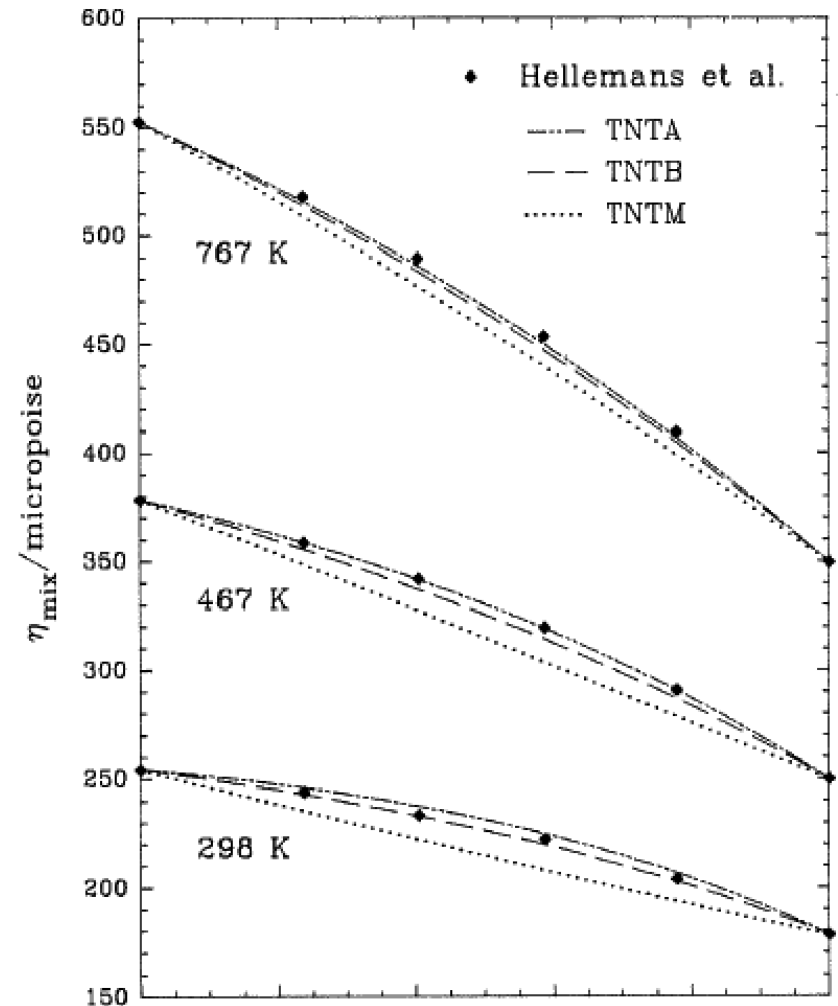
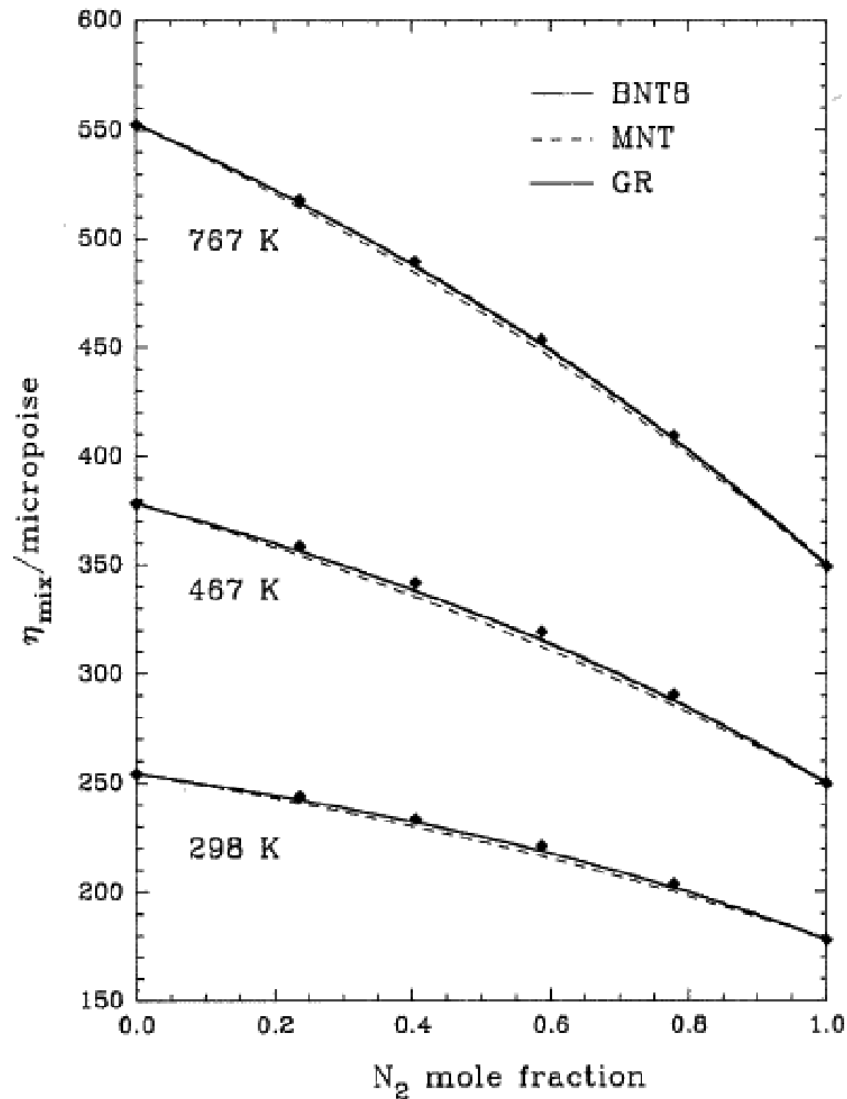
- Classical trajectories on simple model potentials for N₂-Kr. Comparison with relaxation and other data, M.A. ter Horst and C.J. Jameson, J. Chem. Phys. 102, 4431-4446 (1995).
- The N₂-Kr interaction: a multiproperty analysis, F.R.W. McCourt, M.A. ter Horst, and C.J. Jameson, J. Chem. Phys. 102, 5752-5760 (1995).
- A comparative study of CO₂-Ar potential surfaces, M.A. ter Horst and C.J. Jameson, J. Chem. Phys. 105, 6787-6806 (1996)
- A classical dynamics study of the anisotropic interactions in NNO-Ar and NNO-Kr systems. Comparison with transport and relaxation data, M.A. ter Horst and C.J. Jameson, J. Chem. Phys. 109, 10238-10243 (1998)

Different cross sections are sensitive to different parts of the potential function. Simultaneous availability of experimental cross sections for several different observables is necessary to fit a multi-parameter potential function with collision dynamics calculations.

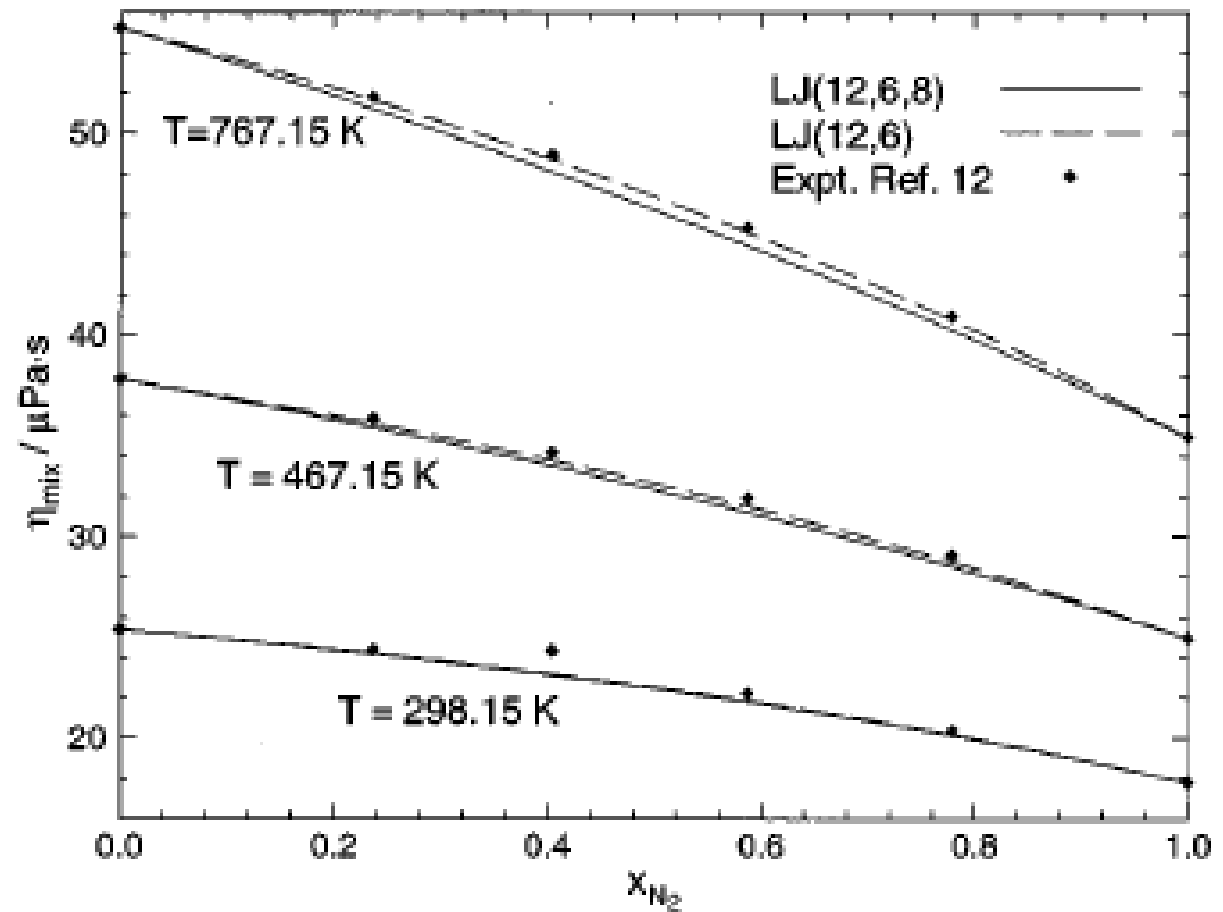
diffusion
in N_2 -Kr
mixtures
from
classical
trajectory
calculations



viscosities for N₂-Kr mixtures from classical trajectories compared with experiment



viscosities for N₂-Kr mixtures from classical trajectories compared with experiment



cross sections for N₂-Kr from classical trajectories compared with experiments

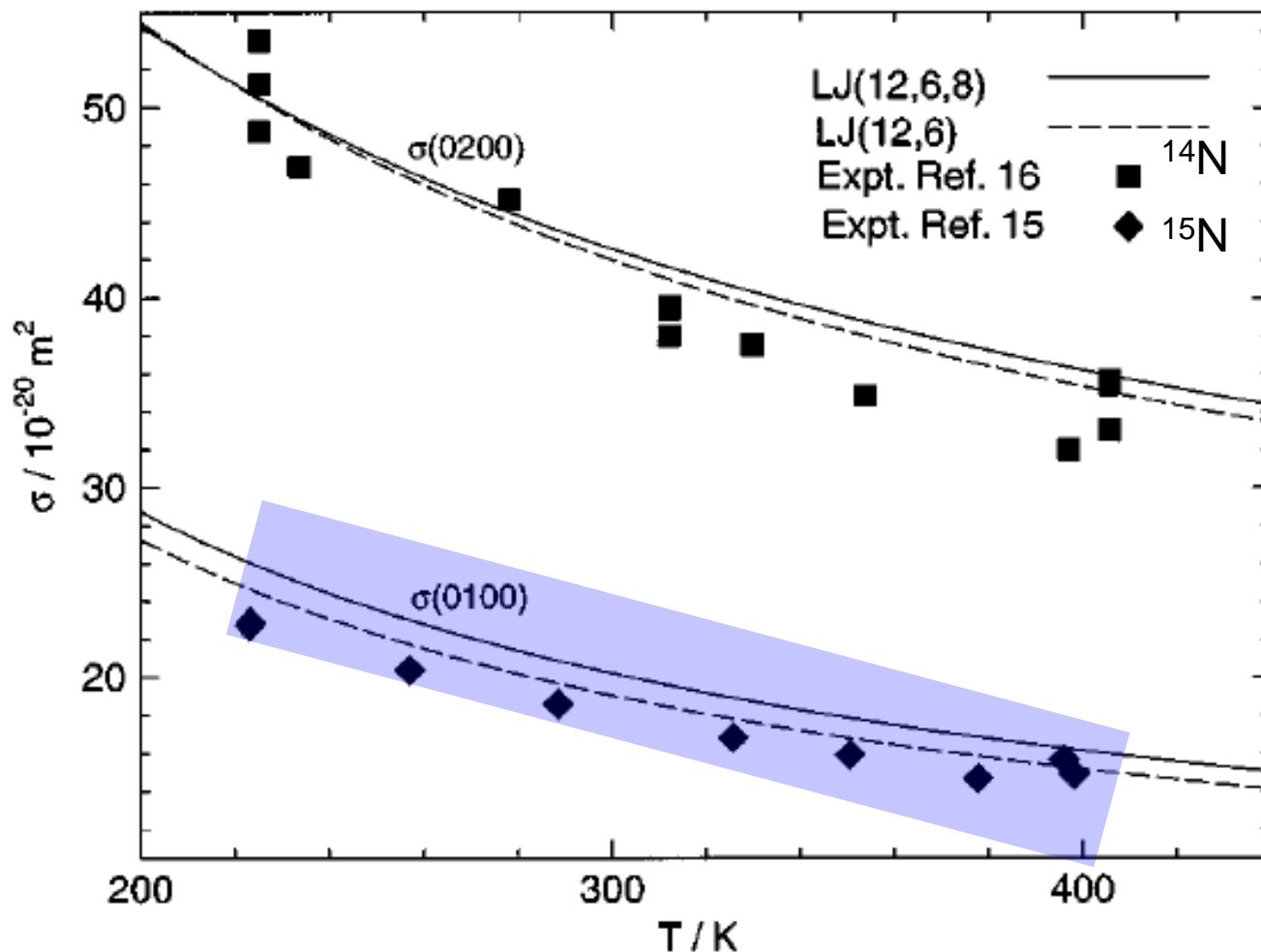
$\sigma(0200)$

or $\sigma_{\theta,2}$
from ¹⁴N

relaxation

$\sigma(0100)$

or σ_J
from ¹⁵N
relaxation

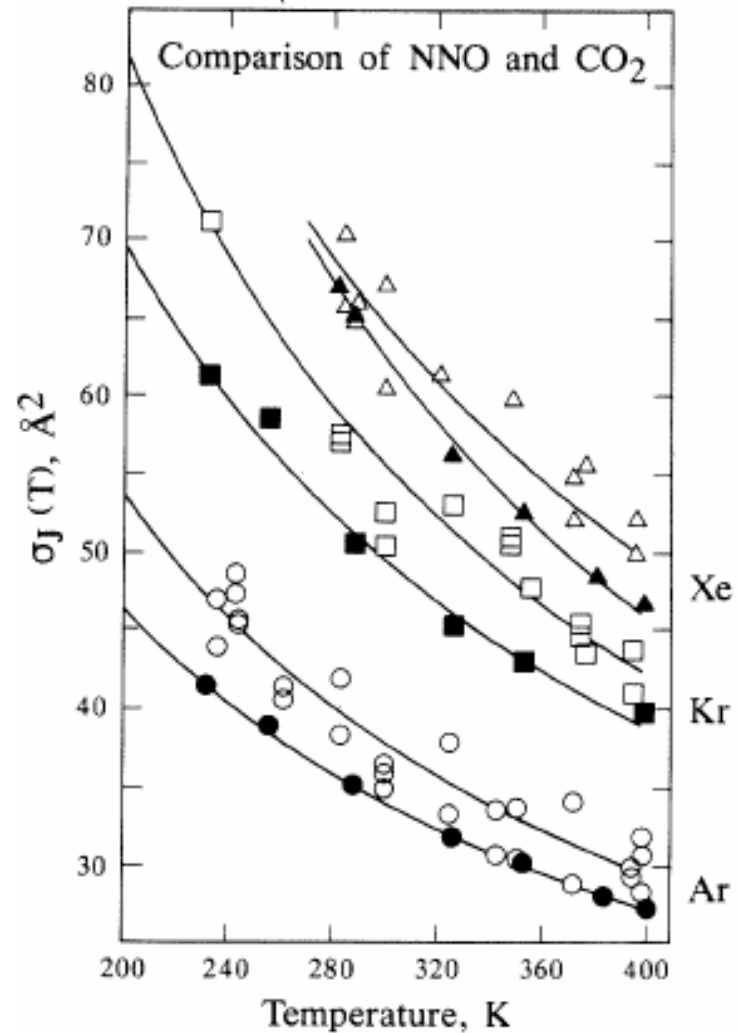


general trends?

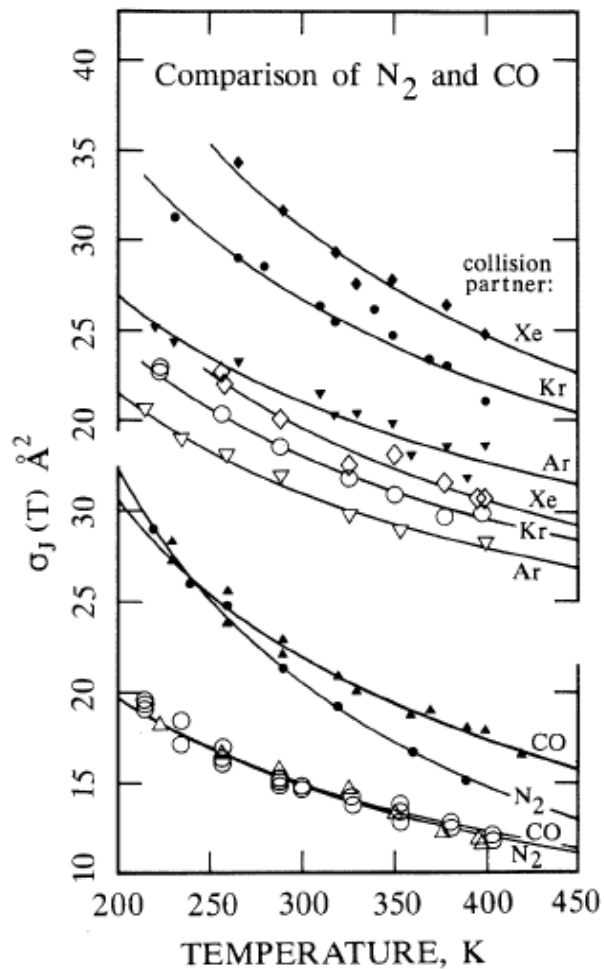
Can we say something about angular momentum relaxation without doing scattering calculations?

- size of the molecules
- anisotropy of the electronic distribution of the probe molecule
- kinematic factors
- the average well depth

NNO and CO₂
have similar
structural anisotropy



N_2 and CO
have similar
structural anisotropy



take size into account: compare ratios of cross section with πd_{ij}^2

using hard sphere diameters d_{ij} to get geometric cross sections

$$\text{collision efficiency} = \sigma_J / \pi d_{ij}^2$$

trends

- Absolute magnitude of efficiency is determined primarily by the **anisotropy of the electronic distribution of the probe molecule.**
- The change of efficiency with increasing mass of buffer (or its number of electrons) is greatest for the SF_6 probe, least for the light molecule probes, esp. CH_4
- The cross section is very intimately connected with details of the potential surface. Nevertheless there is surprisingly high predictive value in the kinematic factors alone

discover factors in cross sections

from our
experiments in
the gas phase

$$\frac{1}{\tau_J} = \rho \bar{v} \sigma_J$$

Compare with
Chandler's
perfectly rough
hard spheres in
the liquid
phase

$$\frac{1}{\tau_J} = \frac{1}{\tau_\omega} = \left(\frac{2I_0}{\mu d^2} + 1 \right)^{-1} \rho \left(\frac{8kT}{\pi\mu} \right)^{1/2} (\pi d^2) \frac{2}{3} g_d(d)$$

This must be the
analog of our $\sigma_J / \pi d_{ij}^2$

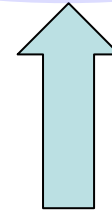
for unlike hard
spheres use
this instead

$$\left[\frac{2I_1}{\mu_{12} d_{11}^2} + \frac{1}{2} \left(1 + \frac{I_1}{I_2} \frac{d_{22}^2}{d_{11}^2} \right) \right]^{-1}$$

$g_d(d)$ is the contact value of the hard-sphere radial distribution function

factors underlying the magnitudes of the cross sections

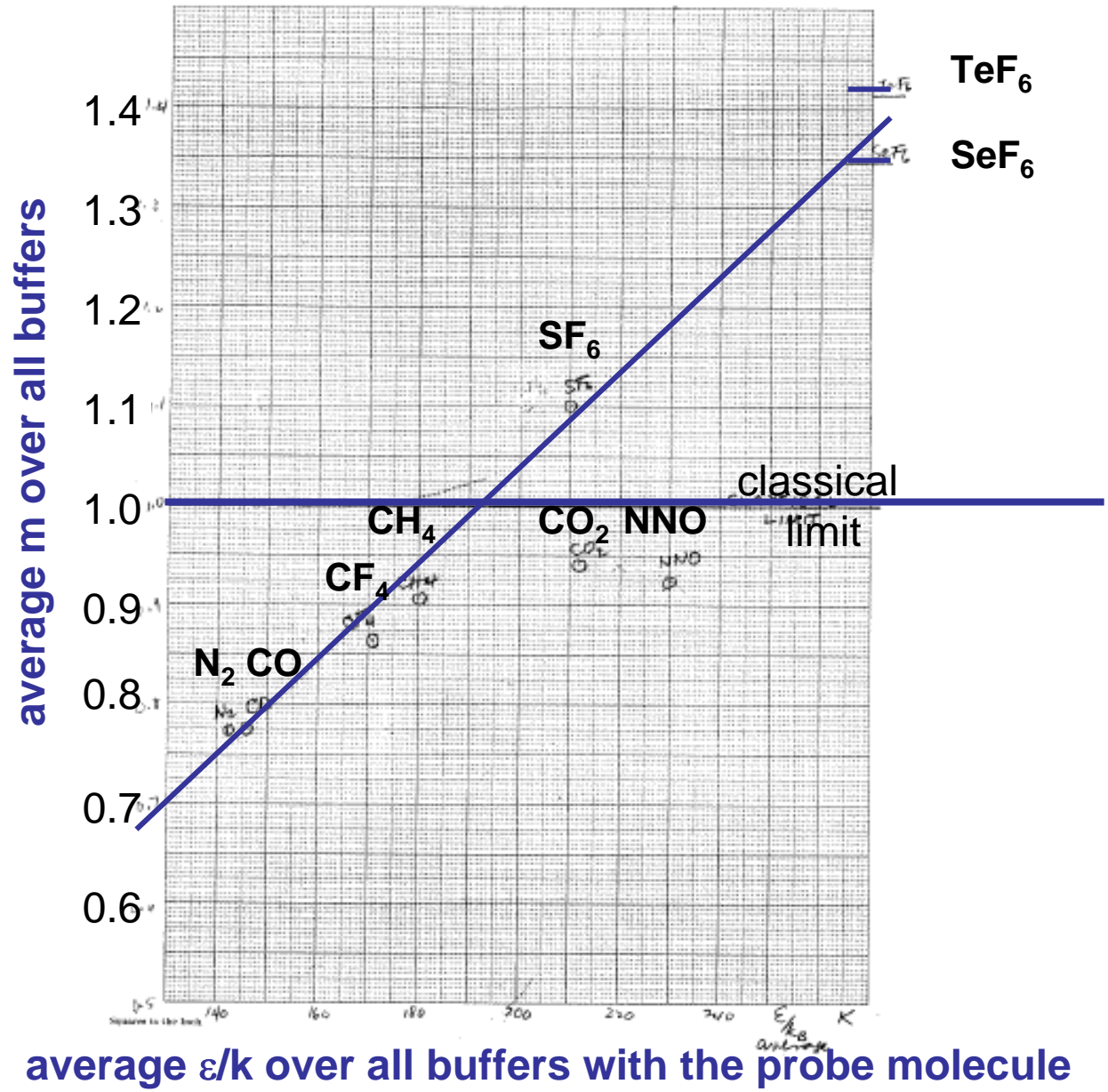
$$\sigma_J \approx (\text{anisotropy factor}) \times \exp^{\epsilon_{12}/kT} \times \left\{ \frac{2I_1}{\mu_{12} d_{11}^2} + \frac{1}{2} \left(1 + \frac{I_1}{I_2} \frac{d_{22}^2}{d_{11}^2} \right) \right\}^{-1}$$



kinematic factors
for collisions between
unlike molecules

trends in the temperature dependence

- For a given probe molecule the power law exponent m in $(T_1/\rho) = (T_1/\rho)_{300K}(T/300)^{-m}$ averaged over all buffers appears to be related to the average well depth
- In the high translational energy limit, m is expected to be 1



CONCLUSIONS

- Relaxation of the rotational angular momentum vector of a molecule can be studied indirectly but quantitatively by NMR
- Collisions between **unlike** molecules can be studied as perfectly as those between like molecules
- The structural anisotropy of the probe molecule is the major determinant of the magnitude of the cross section σ_J
- By studying probe molecules in collision with the same set of 10 other molecules, general factors underlying the magnitudes of the cross sections have been revealed
- The temperature dependences are not all the same i.e., T_1^{SR} does not always go as $T^{-3/2}$, and there is a general increase with the well depth of the collision pair.
- Our classical trajectory calculations in $\text{CO}_2\text{-Ar}$ and $\text{N}_2\text{-Kr}$ give good agreement with a set of thermophysical and relaxation properties of the mixture

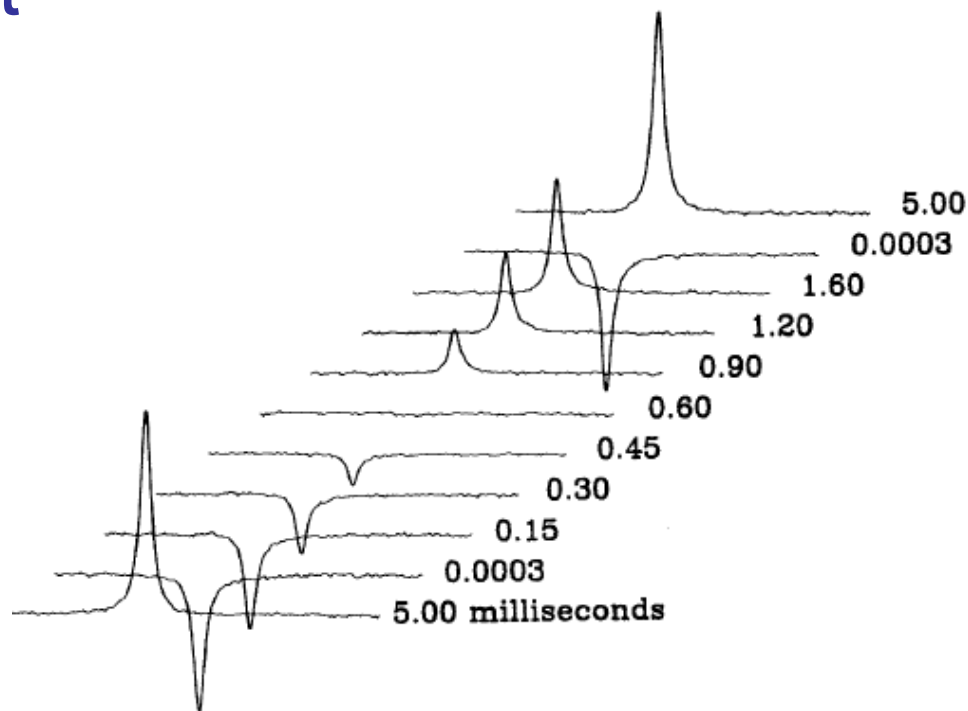
Quadrupolar relaxation in the gas phase

^{14}N in N_2 in 10 gases

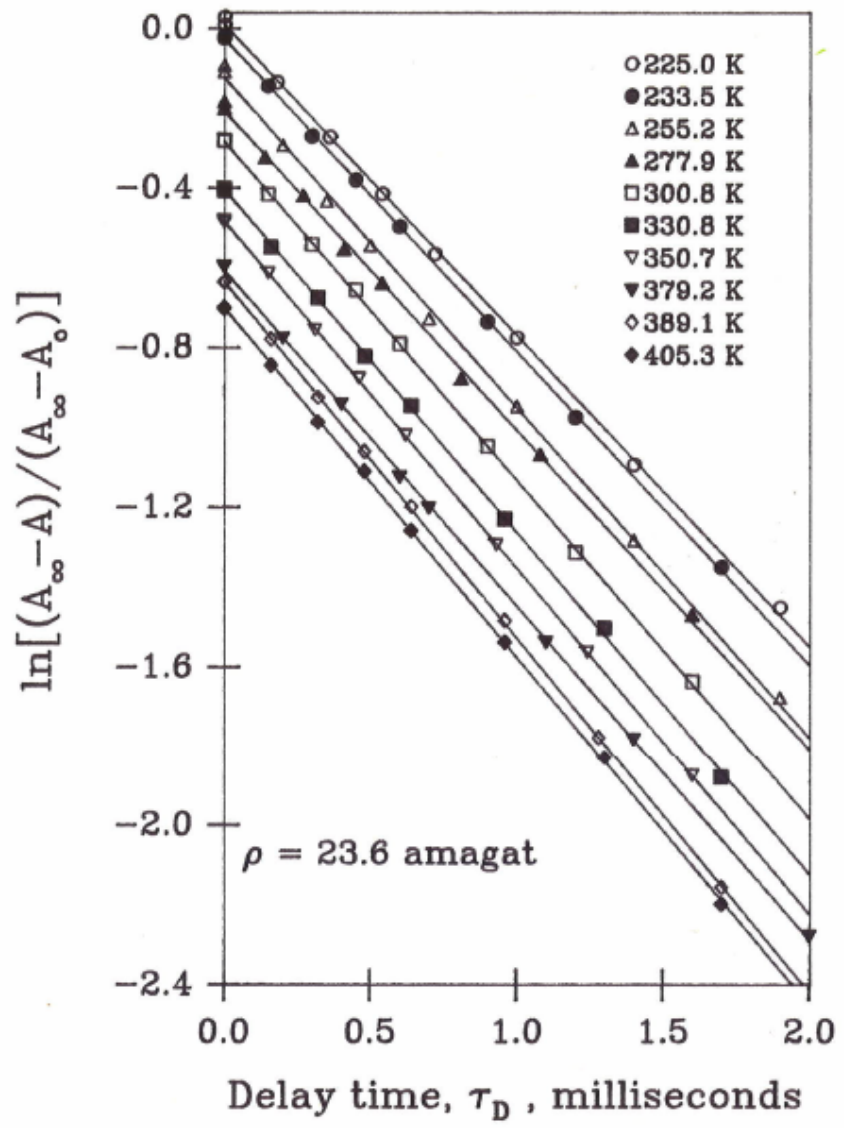
^{14}N in $^{14}\text{N}^{14}\text{NO}$ in 10 gases

^2D in CD_4 in 10 gases

a typical T_1
experiment

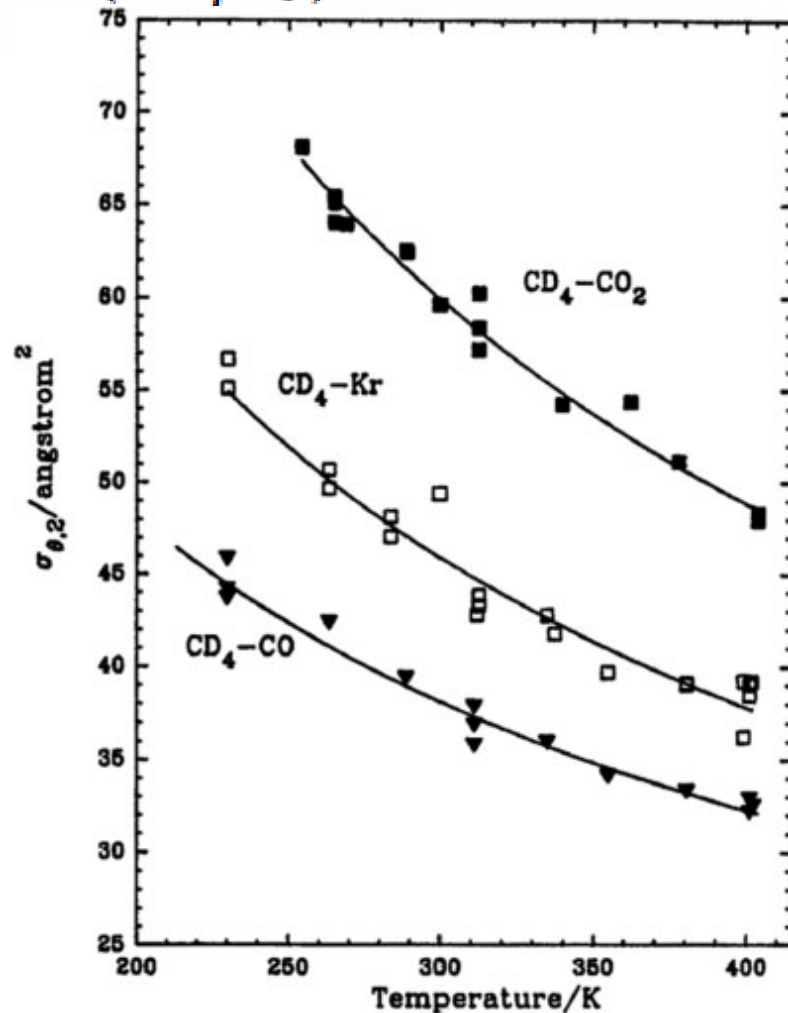


^{14}N inversion recovery in $^{14}\text{N}_2$ gas



cross sections for molecular reorientation, $\sigma_{\theta,2}$

$$T_1^Q = \frac{200}{3} \frac{I^2(2I-1)}{(2I+3)} \left(\frac{\hbar}{e^2 q Q} \right)^2 \rho \langle v \rangle \sigma_{\theta,2}$$

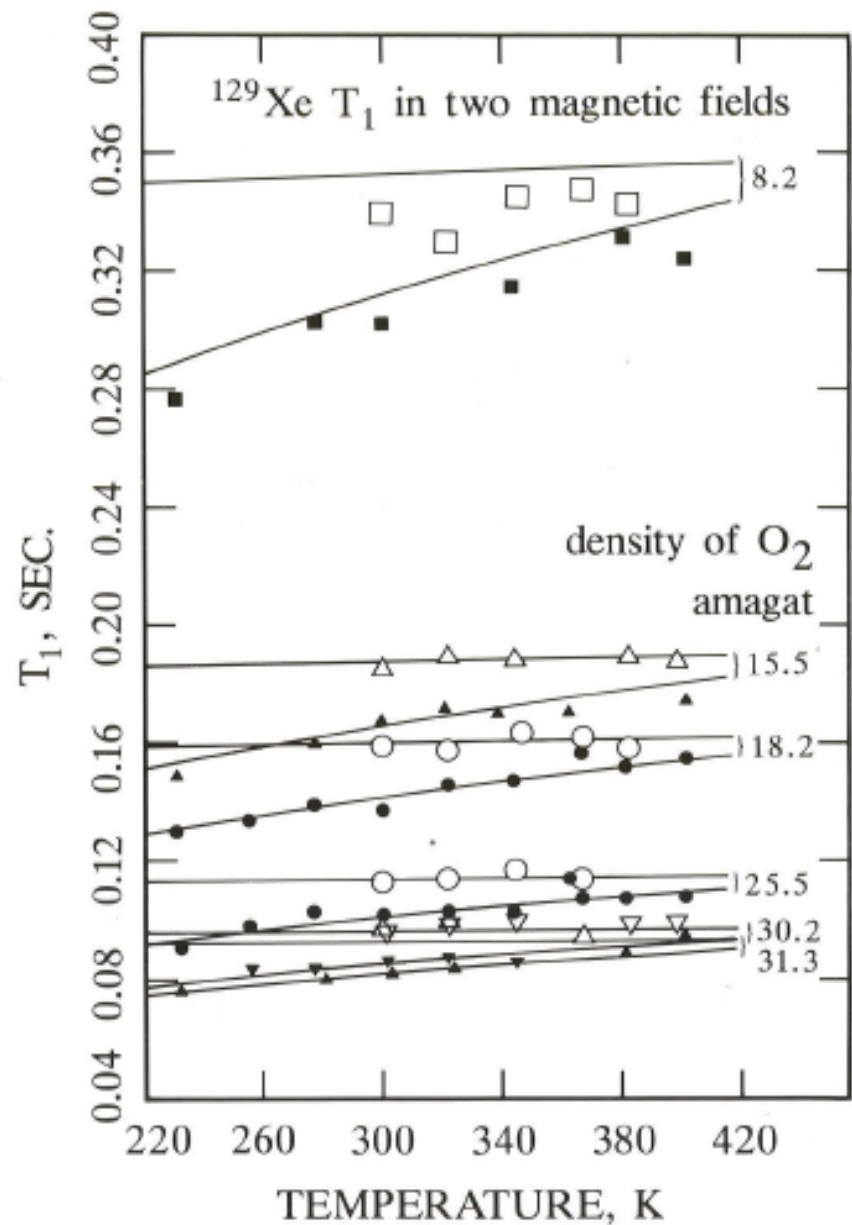


Intermolecular dipole-dipole (nuclear spin dipole-electron spin dipole) relaxation

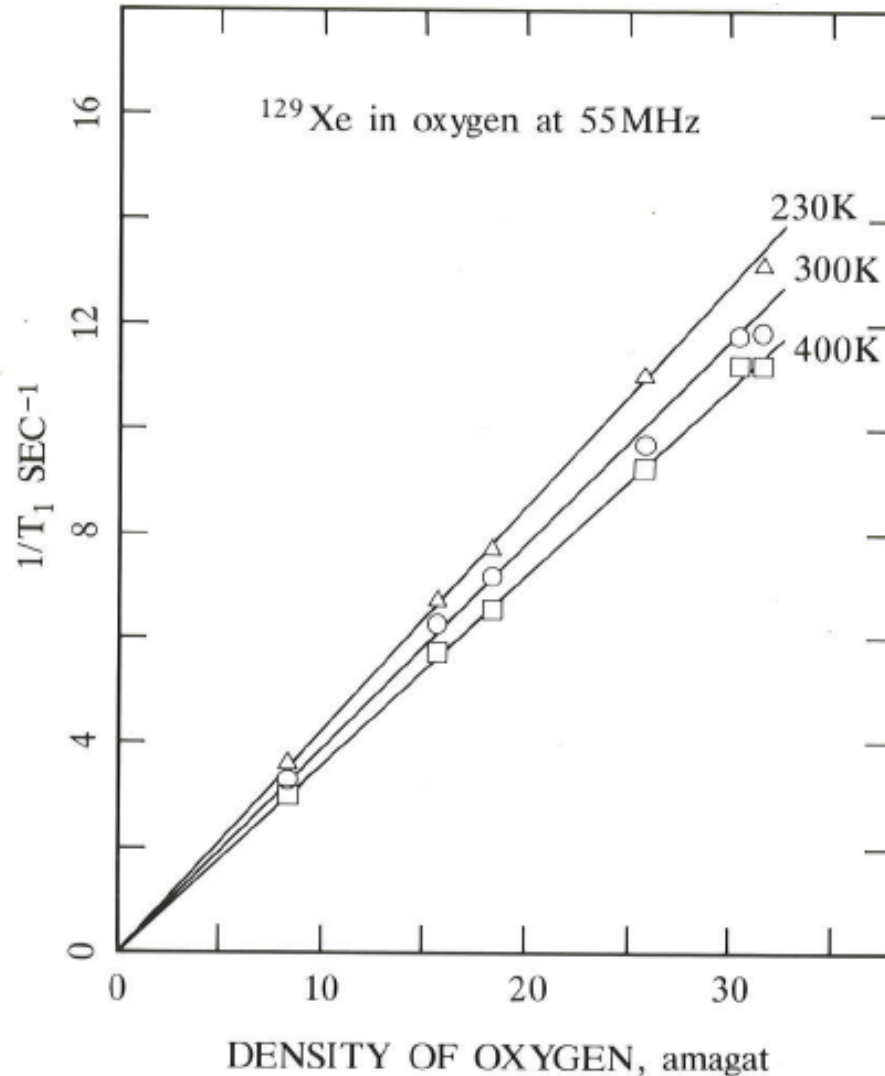
of ^{129}Xe , ^{19}F in CF_4 , SF_6 , SeF_6 ,
 TeF_6 , ^1H in CH_4 in O_2 gas

relaxation studies of ^{129}Xe in O_2

in two magnetic fields

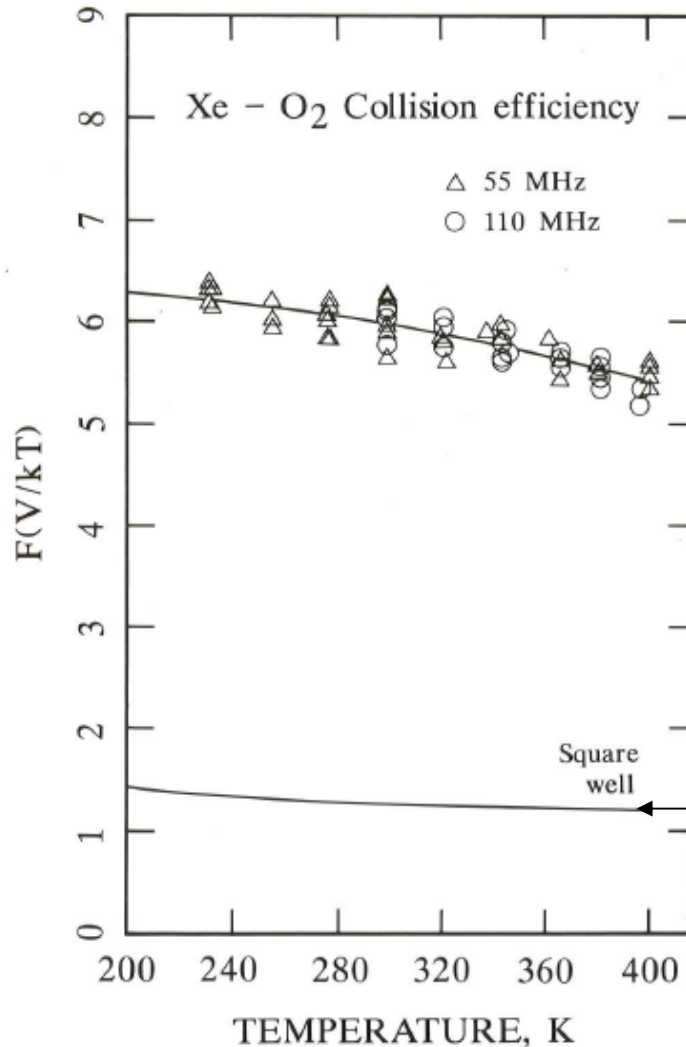


^{129}Xe relaxation is dominated by Xe-O_2 collisions



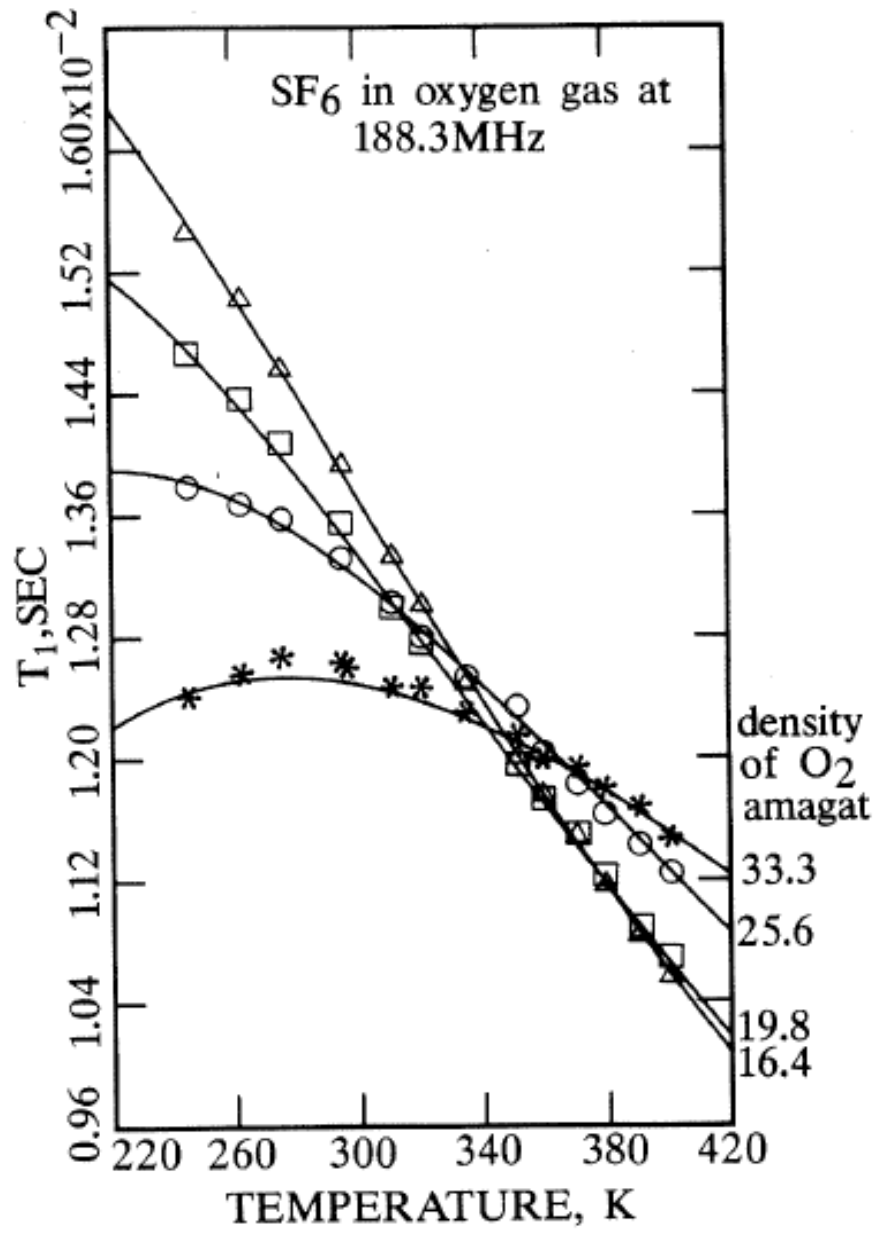
collision efficiencies for ^{129}Xe spin relaxation in O_2

very sensitive
to the form of the
intermolecular
potential

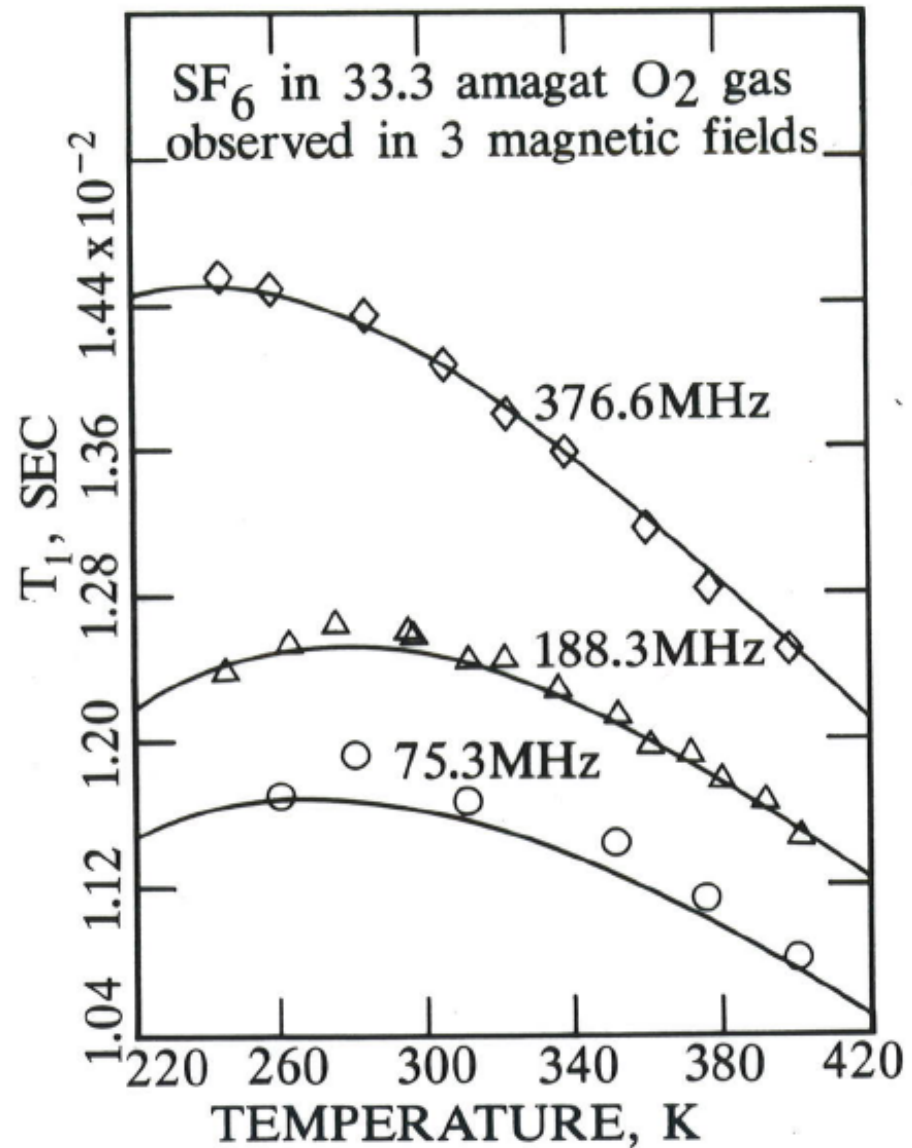


collision
efficiency
calculated for
a square well
potential

relaxation studies of ^{19}F for SF_6 in O_2

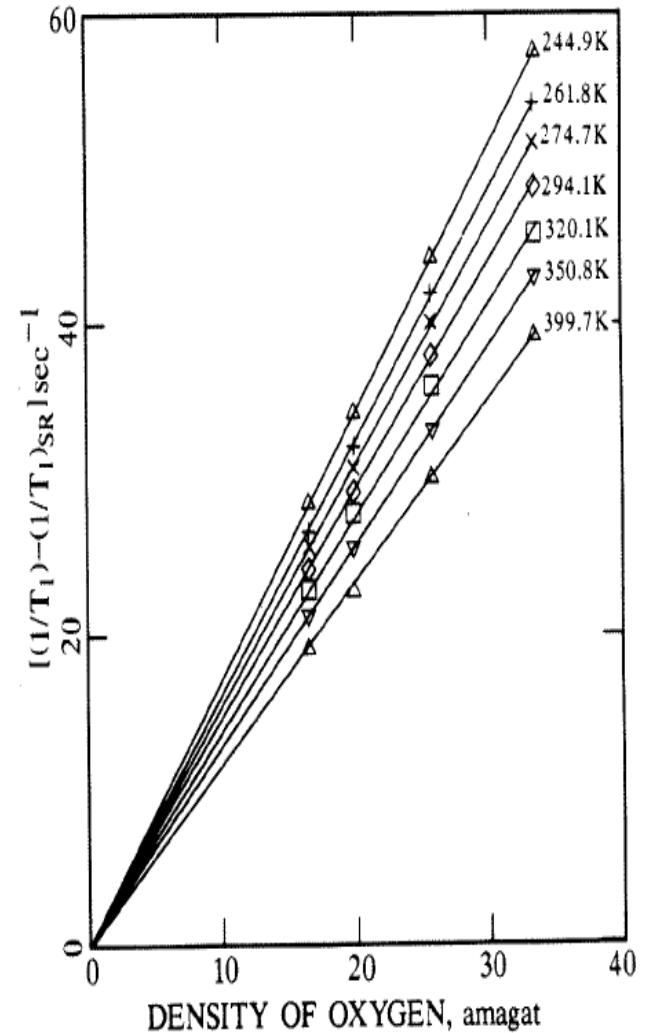


measure T_1 in 3 magnetic fields



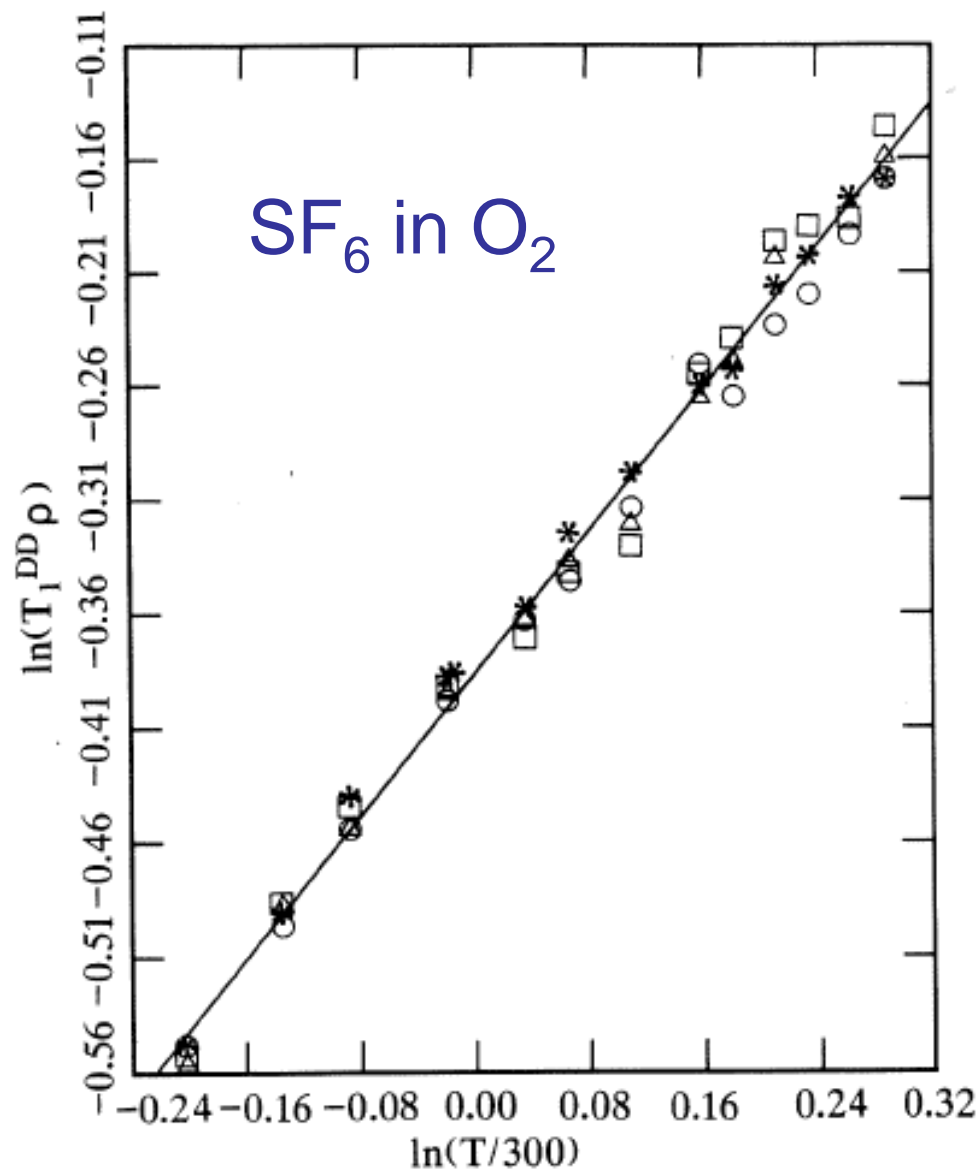
separation of spin rotation contributions to find T_1 DD

$\left(\frac{T_1}{\rho}\right)_{SF_6-SF_6}^{SR}$ was obtained from pure SF_6 gas studies, but $\left(\frac{T_1}{\rho}\right)_{SF_6-O_2}^{SR}$ had to be determined. This value is obtained by iteration. When the correct value is arrived at, the remaining relaxation rate must behave according to $\frac{1}{T_1} \propto \rho_{O_2}$ at each temperature at all three fields



temperature dependence of $T_1^{DD} \rho_{O_2}$

all samples
at one
magnetic field



factors in T_1^{DD}

For a hard sphere potential in the limit of zero magnetic field:

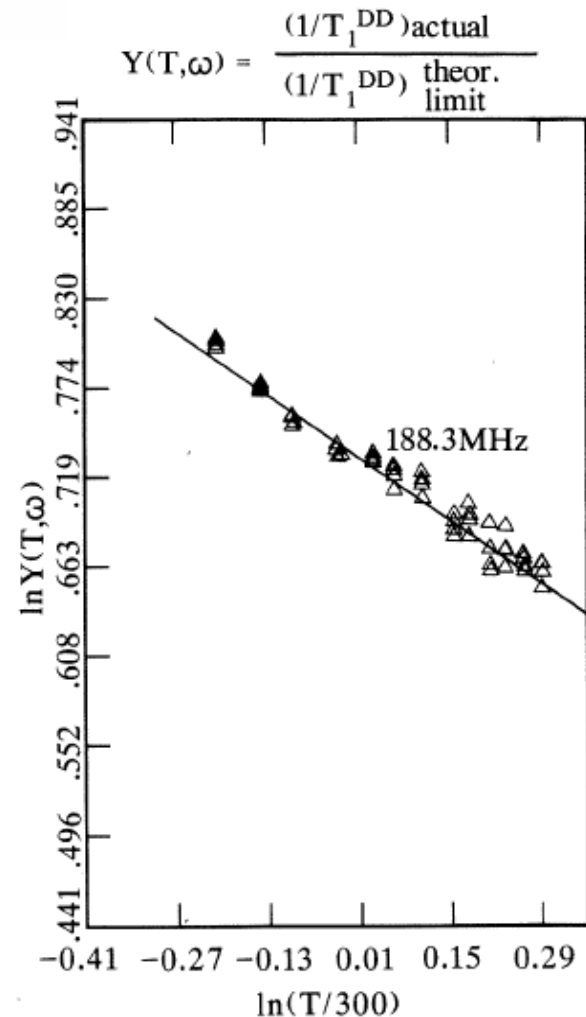
$$\left(\frac{1}{T_1^{\text{DD}}}\right)_{\text{theor.lim.}} = \frac{16}{3} S(S+1) \gamma_I^2 \gamma_S^2 \frac{\hbar}{d^2} \left(\frac{\pi\mu}{8kT}\right)^{1/2} N_S$$

$$\frac{1}{T_1^{\text{DD}}} = F(V/kT) \{1 - f(T)\sqrt{\omega_I}\} \left(\frac{1}{T_1^{\text{DD}}}\right)_{\text{theor.lim.}}$$

Measurements in more than one magnetic field permits determination of $f(T)$ and then $F(V/kT)$. All information about the intermolecular potential is in the collision efficiency $F(V/kT)$.

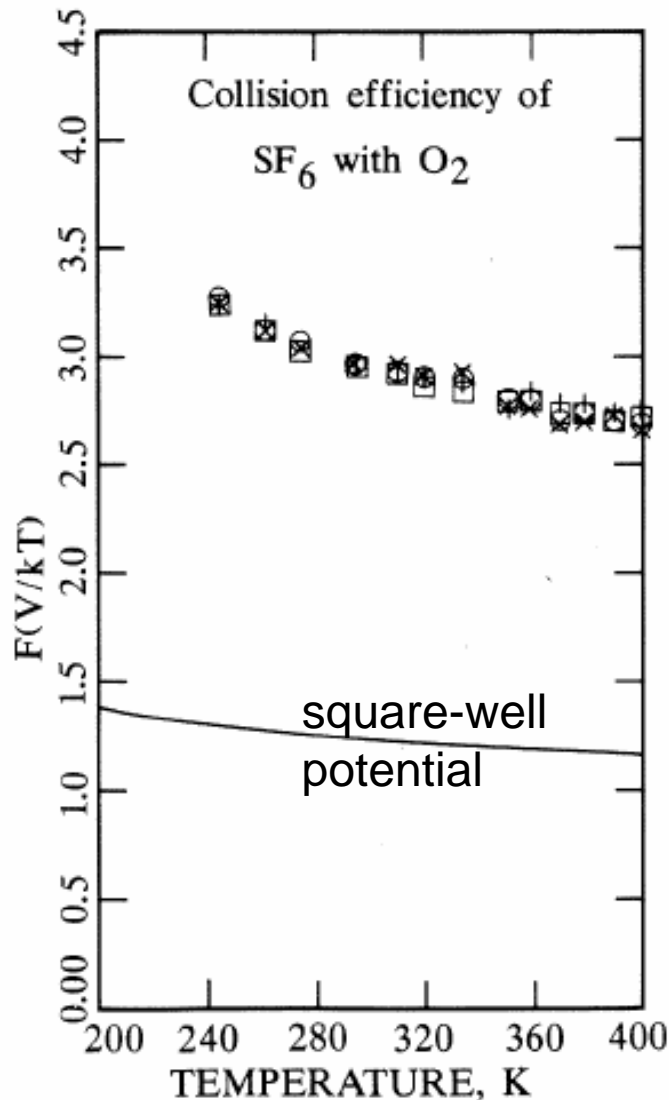
$$Y(T, \omega) = \frac{(1/T_1^{DD})_{\text{actual}}}{(1/T_1^{DD})_{\text{theor. limit}}}$$

The theoretical expression for $\frac{1}{T_1^{DD}}$ for a hard sphere potential, at the high translational energy limit, zero field limit ($\omega=0$), is known. Our measured dipolar relaxation rates divided by the theoretical limit are shown in Fig. 6 for one sample. These values contain the effects of the intermolecular potential, V , and the magnetic field; theoretical arguments predict that in the dilute gas the first will be a function of V/kT and that in the low frequency limit the second is of the form $(1 - f(T) \sqrt{\omega})$. Thus, Fig. 6 shows $F(V/kT)(1 - f(T) \sqrt{\omega})$ if our theory is correct.

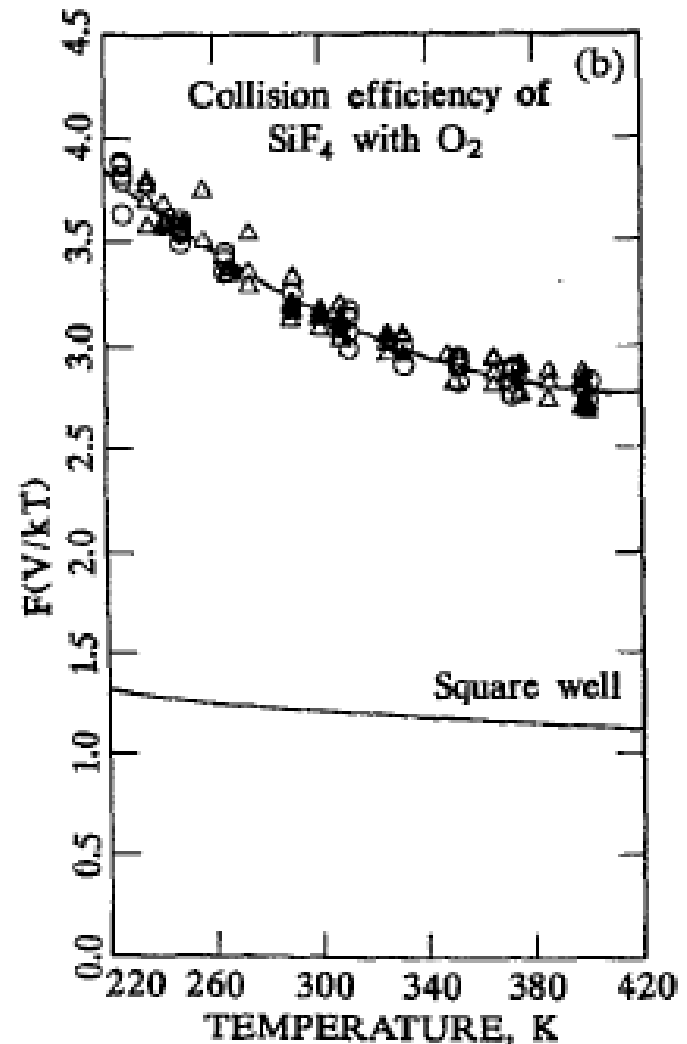
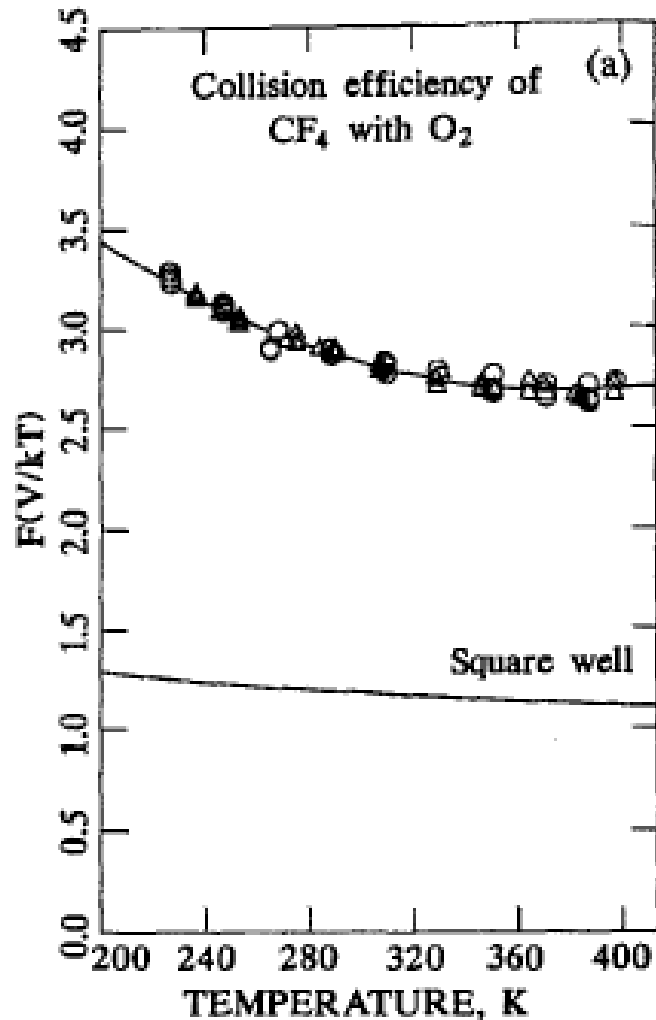


divide out ω -dependence to find dependence on the intermolecular potential

great sensitivity to the form of the intermolecular potential!



collision efficiencies for $\text{CF}_4\text{-O}_2$ and $\text{SiF}_4\text{-O}_2$



CONCLUSIONS

- We have characterized nuclear spin relaxation rate due to the **dipole-electron spin dipole mechanism**
- This relaxation rate is factorable into:
 - the density of O₂
 - the theoretical limit field-dependent & temperature-dependent term
 - the temperature dependent interesting factor which depends on the intermolecular potential
- Comparison of last factor with the results for a square-well potential shows the great sensitivity of T_1^{DD} to the form of the intermolecular potential

ACKNOWLEDGMENT



**A. Keith Jameson
Joseph K. Hwang (UG)
Marc A. ter Horst
Nancy C. Smith
Diane C. Dabkowski (UG)
Karol Jackowski**

***and trajectory
calculations with
R. F. W. McCourt***